The Plant Cell, Vol. 19: 2822–2838, September 2007, www.plantcell.org © 2007 American Society of Plant Biologists

INCURVATA2 Encodes the Catalytic Subunit of DNA Polymerase α and Interacts with Genes Involved in Chromatin-Mediated Cellular Memory in *Arabidopsis thaliana*

José María Barrero,[a,1] Rebeca González-Bayón,[a] Juan Carlos del Pozo,[b] María Rosa Ponce,[a] and José Luis Micol[a,2]

[a] División de Genética and Instituto de Bioingeniería, Universidad Miguel Hernández, 03202 Elche, Alicante, Spain
[b] Instituto Nacional de Investigación y Tecnología Agraria y Alimentaria, Departamento de Biotecnología, 28040 Madrid, Spain

Cell type–specific gene expression patterns are maintained by the stable inheritance of transcriptional states through mitosis, requiring the action of multiprotein complexes that remodel chromatin structure. Genetic and molecular interactions between chromatin remodeling factors and components of the DNA replication machinery have been identified in *Schizosaccharomyces pombe*, indicating that some epigenetic marks are replicated simultaneously to DNA with the participation of the DNA replication complexes. This model of epigenetic inheritance might be extended to the plant kingdom, as we report here with the positional cloning and characterization of *INCURVATA2* (*ICU2*), which encodes the putative catalytic subunit of the DNA polymerase α of *Arabidopsis thaliana*. The strong *icu2-2* and *icu2-3* insertional alleles caused fully penetrant zygotic lethality when homozygous and incompletely penetrant gametophytic lethality, probably because of loss of DNA polymerase activity. The weak *icu2-1* allele carried a point mutation and caused early flowering, leaf incurvature, and homeotic transformations of sepals into carpels and of petals into stamens. Further genetic analyses indicated that *ICU2* interacts with *TERMINAL FLOWER2*, the ortholog of *HETEROCHROMATIN PROTEIN1* of animals and yeasts, and with the Polycomb group (PcG) gene *CURLY LEAF*. Another PcG gene, *EMBRYONIC FLOWER2*, was found to be epistatic to *ICU2*. Quantitative RT-PCR analyses indicated that a number of regulatory genes were derepressed in the *icu2-1* mutant, including genes associated with flowering time, floral meristem, and floral organ identity.

INTRODUCTION

Organogenesis depends on cell fate decisions that must be maintained through the cell divisions that lead to the adult body of multicellular organisms. Such maintenance requires the stable inheritance of gene expression states and behaves as a cellular memory that allows the determined cells to retain their developmental identity through successive mitotic cycles (Schubert et al., 2005). Loss of such cellular memory causes diverse developmental aberrations and diseases, including cancer (Rountree et al., 2001; Gil et al., 2005).

Certain small RNAs are involved in initiating the heterochromatinization of specific chromosome regions (Grewal and Moazed, 2003; Zilberman et al., 2003; Craig, 2004; Lippman and Martienssen, 2004; Mathieu and Bender, 2004). After initiation, protein complexes are recruited that introduce epigenetic marks in histones. Methylation of H3K9 (the Lys-9 residue of the N-terminal tail of the H3 histone) is the most widely studied of these epigenetic marks and seems to be an essential element in the heterochromatinization process (Soppe et al., 2002; Elgin and Grewal, 2003; Craig, 2004). Methylated H3K9 is recognized by the Heterochromatin protein 1 (HP1) of *Drosophila melanogaster* (Bannister et al., 2001) and its orthologs, Switching 6 (Swi6) of *Schizosaccharomyces pombe* and the human HP1 (Lachner et al., 2001). After its binding to methylated histones, HP1 mediates the recruitment of other proteins to assemble multiprotein complexes with histone methyltransferase activity (Fransz and de Jong, 2002; Craig, 2004), which repress gene expression through the formation of higher-order chromatin structures (Grewal and Elgin, 2002). During S phase, these structures need to be removed to allow DNA replication and then quickly reassembled to maintain the gene expression states.

The Polycomb group (PcG) of repressors includes crucial components of cellular memory mechanisms that rely on the inheritance of modifications in specific histone tails. They were first discovered in *D. melanogaster* and found to be responsible for the maintenance of early determined transcription patterns throughout the life cycle of the fly. Loss-of-function mutations in PcG genes result in ectopic expression of homeotic genes (Paro et al., 1998; Francis and Kingston, 2001; Cunliffe, 2003). PcG genes encode components of multiprotein complexes that catalyze methylation of the N-terminal tail of the H3 and H4 histones (Peterson and Laniel, 2004).

Chromatin-mediated gene repression systems exist in plants (He and Amasino, 2005), where an *HP1* homolog and several PcG genes have been described. The only protein of *Arabidopsis thaliana* with overall sequence similarity to HP1 is TERMINAL

[1] Current address: Commonwealth Scientific and Industrial Research Organization Plant Industry, GPO Box 1600, ACT 2601 Canberra, Australia.
[2] Address correspondence to jlmicol@umh.es.
The author responsible for distribution of materials integral to the findings presented in this article in accordance with the policy described in the Instructions for Authors (www.plantcell.org) is: José Luis Micol.
www.plantcell.org/cgi/doi/10.1105/tpc.107.054130

FLOWER2 (TFL2; also known as LIKE HETEROCHROMATIN PROTEIN1; Larsson et al., 1998; Gaudin et al., 2001; Turck et al., 2007). TFL2 acts as a repressor of genes involved in flowering time, floral organ identity, meiosis, and seed maturation (Nakahigashi et al., 2005). TFL2 is a euchromatic protein that mainly associates with regions evenly distributed along euchromatin, each covering one or two genes marked by the trimethylated H3K27 repressive mark (Turck et al., 2007).

The PcG genes identified in *Arabidopsis* include, among others, *CURLY LEAF* (*CLF*; Goodrich et al., 1997), which represses the floral organ identity gene *AGAMOUS* (*AG*; Yanofsky et al., 1990) throughout plant development, *VERNALIZATION2* (*VRN2*; Gendall et al., 2001), which is required for the maintenance of the repression of *FLOWERING LOCUS C* (*FLC*; Bastow et al., 2004) in response to vernalization, and *EMBRYONIC FLOWER2* (*EMF2*; Yoshida et al., 2001), which is required to maintain vegetative development and represses flower development (Moon et al., 2003). It has been proposed that different PcG complexes exist in plants, which would include common components, such as EMF2, and specific components, such as CLF and VRN2 (Otte and Kwaks, 2003; Reyes and Grossniklaus, 2003; Chanvivattana et al., 2004). Loss-of-function alleles of the *CLF* and *EMF2* PcG genes share a pleiotropic phenotype that include leaf curling, early flowering, and the misexpression of many genes, some of which encode transcription factors (reviewed in Reyes, 2006). Some of these phenotypic traits are also caused by mutations in genes that encode putative chromatin remodeling factors, such as *TFL2*, *EARLY BOLTING IN SHORT DAYS* (Piñeiro et al., 2003), and *SPLAYED* (Wagner and Meyerowitz, 2002), and by the silencing of *BRAHMA* (Farrona et al., 2004).

We have already studied at a preliminary level the *incurvata2-1* (*icu2-1*) mutant, which displayed mildly incurved leaves and early flowering. It was identified in a study of 152 *Arabidopsis* mutants with abnormally shaped leaves, which belong to the Arabidopsis Information Service Form Mutants collection, 13 of which had been isolated by G. Röbbelen and displayed curled, involute leaves, a phenotype that we named Incurvata (Serrano-Cartagena et al., 1999). We found the *icu* mutations to belong to five complementation groups, one of which, *ICU2*, was represented by a single recessive allele, *icu2-1*, which caused the ectopic derepression of several floral organ identity genes in the leaves. In addition, the *icu2-1 clf* double mutants displayed a synergistic phenotype. Taken together, our results suggested a functional relationship between the *ICU2* gene and PcG-mediated gene repression (Serrano-Cartagena et al., 2000).

Here, we report the positional cloning of the *ICU2* gene, which was found to encode the putative catalytic subunit of DNA polymerase α, and the isolation of lethal *icu2* alleles. The morphological and molecular phenotypes caused by the *icu2* mutations, the molecular nature of the *icu2-1* allele, and its genetic interactions with mutations in *TFL2* and several PcG genes suggest a role for the replication machinery in epigenetic inheritance and plant chromatin packaging. Our results suggest the existence in plants of a cellular memory mechanism that involves DNA polymerase α, as proposed by previous authors for the fission yeast (Nakayama et al., 2000, 2001; Ahmed et al., 2001; Vermaak et al., 2003).

RESULTS

The Recessive *icu2-1* Mutation Causes Leaf Incurvature, Early Flowering, and Homeotic Floral Transformations

The phenotype of the *icu2-1* mutant is pleiotropic. Its vegetative leaves were of slightly reduced size and displayed some bilateral asymmetry and a variable degree of incurvature (Figures 1A and 1B). The surface of these leaves was uneven, which correlated with the presence of patches of small epidermal cells (Figures 1C and 1D). The *icu2-1* mutant showed reduced apical dominance, developing an increased number of secondary stems, and its flowers displayed partial homeotic transformations of sepals into carpels and of petals into stamens (Figure 1E). These flower aberrations are similar to those shown by mutants carrying loss-of-function *apetala2* alleles, which derepress *AG* in the first and second floral whorls (Bowman et al., 1989). The *icu2-1* mutant was early flowering, bolting 24.43 $\pm$ 2.10 d after sowing (the wild-type Enkheim-2 [En-2] bolted 37.80 $\pm$ 2.90 d after sowing) and produced less vegetative leaves (9.36 $\pm$ 0.81) than En-2 (12.40 $\pm$ 0.52).

The *ICU2* Gene Encodes the Catalytic Subunit of DNA Polymerase α

We previously mapped the *icu2-1* mutation at a low-resolution level to the lower arm of chromosome 5, linked to the nga129 and MBK5 microsatellites (Serrano-Cartagena et al., 2000). Further linkage analyses allowed us to define a 50-kb candidate region (Figure 2A), which encompassed 15 annotated genes. All the putative transcription units within the candidate region were sequenced in *icu2-1*/*icu2-1* and En-2 plants. A missense mutation was found in the At5g67100 gene (Figures 2A and 2B), which encodes the catalytic subunit of the DNA polymerase α of *Arabidopsis*.

To confirm that loss of function of the At5g67100 gene causes the mutant phenotype of *icu2-1*/*icu2-1* plants, a transgene-mediated complementation experiment was performed. A wild-type (En-2) genomic fragment of 9467 bp encompassing the entire region between the At5g67090 and At5g67110 genes was cloned into the pGreenII0179 vector. The resulting construct was named *pG-ICU2* and transferred into *icu2-1*/*icu2-1* plants (see Methods). Nine transformant lines were obtained, all of which displayed wild-type morphology (Figure 3A).

At5g67100 is a large, single-copy gene that contains 30 exons, coding for a 1492–amino acid protein (Figure 2B). The *icu2-1* mutation consisted of a C$\rightarrow$T transition in the 24th exon of At5g67100, in nucleotide position 6762 of the transcription unit (numbering from the initiation codon), which substituted Arg by Cys in amino acid position 1273 (Figure 2B), a residue that is outside the predicted polymerase catalytic domains of the enzyme (see the II, III, and V domains in Figure 2B; Wong et al., 1998) and other conserved regions. The promoter of this gene includes the E2F binding site motif TTTCCCGC, which is characteristic of cell cycle–regulated genes (Fry and Farnham, 1999; Chaboute et al., 2000).

Proteins interacting with HP1 in *D. melanogaster* share the PXVXL consensus sequence, named the MOD1-interacting

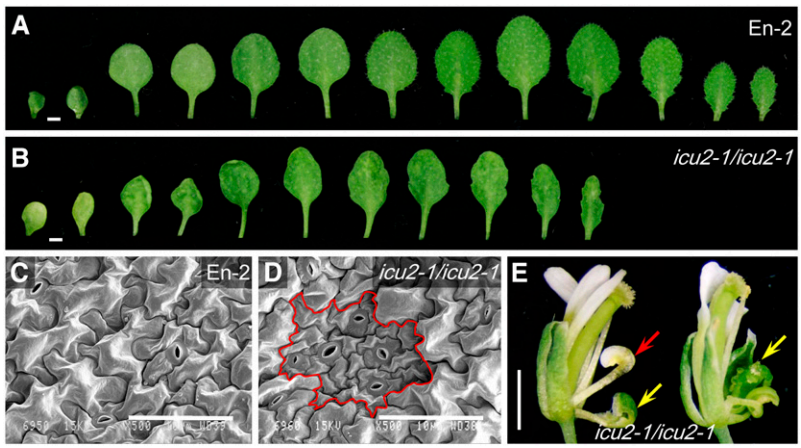

Figure 1. Leaf and Flower Phenotypic Traits of the *icu2-1* Mutant.

(A) and **(B)** Excised cotyledons (left) and leaves.
(C) and **(D)** Scanning electron micrographs of the central region of the adaxial surface of third node leaf laminae (obtained as described in Serrano-Cartagena et al., 2000).
(E) Flowers.
(A) and **(C)** The En-2 wild type.
(B), **(D)**, and **(E)** *icu2-1/icu2-1* plants.
A patch of epidermal cells with reduced size is highlighted in **(D)**. Arrows in **(E)** indicate partial homeotic transformations of sepals into carpels (yellow) and petals into stamens (red). Bars = 1 mm in **(A)**, **(B)**, and **(E)** and 100 μm in **(C)** and **(D)**.

region (MIR) domain (Murzina et al., 1999; Smothers and Henikoff, 2000). A similar pentameric sequence (PFVQV) is present in Swi7, the DNA polymerase α of *S. pombe*, and is required for its binding to the HP1 homolog Swi6 (Nakayama et al., 2001). This sequence is also shared by other DNA polymerase α proteins, including ICU2 (PHVQV; Figure 2B) and those of *D. melanogaster* (PHVQV) and mammals (PHVHV). A computer-based prediction of protein structure suggested that the amino acid change caused by the *icu2-1* mutation (Figures 2C and 2D) would reduce or abolish access of some proteins to the MIR domain of ICU2.

The *icu2-2* and *icu2-3* Recessive Alleles Cause Early Lethality

A search for insertional alleles of *ICU2* in public collections allowed us to find the GK-731A12 line in the GABI-Kat database (Li et al., 2003; Rosso et al., 2003), which was confirmed as carrying a T-DNA (Sul^r) insertion in position 1075 bp (numbering from the initiation codon) in the first exon of the *ICU2* gene, and named *icu2-2* (Figures 2A and 2B). An enhancer trap line (N175161) that had been generated by J. Clarke and M. Bevan was confirmed as carrying a *Ds* (Kan^r) transposable element in the first exon of the *ICU2* gene and named *icu2-3* (Figures 2A and 2B). The presence of *Ds*- or T-DNA–tagged read-through transcripts was tested by nonquantitative RT-PCR in *ICU2/icu2-2* and *ICU2/icu2-3* heterozygotes, with only the *icu2-3* chimeric transcript being detected.

The *ICU2/icu2-2* and *ICU2/icu2-3* heterozygotes were phenotypically wild-type. No homozygous mutants were found in their progeny, which suggested recessive lethality. We did not find *icu2-1/icu2-2* or *icu2-2/icu2-3* heterozygous plants in the progeny of *icu2-1/icu2-1* × *ICU2/icu2-2* or *ICU2/icu2-2* × *ICU2/icu2-3* crosses, respectively. On the contrary, the *icu2-1/icu2-3* heterozygotes were viable and displayed a morphological phenotype indistinguishable from that of the *icu2-1/icu2-1* homozygotes (Figure 3B). Moreover, the *icu2-2* allele was not transmitted to the viable progeny of reciprocal *icu2-1/icu2-1* × *ICU2/icu2-2* crosses (Table 1).

When developing siliques were dissected in selfed *ICU2/icu2-2* plants, half of the seeds were found to be abnormal, small, and white and seemed to be aborted or unfertilized ovules without any visible embryonic structure (Figures 3C to 3E), whereas all the remaining seeds were morphologically normal, and only 15% of which carried the *icu2-2* allele (Table 1). The siliques of *ICU2/ICU2* × *ICU2/icu2-2* reciprocal crosses displayed aborted or unfertilized ovules and mature seeds, some of which gave morphologically wild-type *ICU2/icu2-2* plants. Our results indicate that most of the female *icu2-2* gametes are not viable and that some wild-type ovules yield lethal zygotes after fertilization by *icu2-2* pollen.

The *icu2-3* allele also caused gametic lethality with incomplete penetrance, although weaker than that of *icu2-2*. This conclusion was reached from analyses of the progeny of selfed *ICU2/icu2-3* plants and those of *ICU2/ICU2* × *ICU2/icu2-3* reciprocal crosses. The corresponding siliques displayed a higher proportion of normal seeds, together with aborted or unfertilized ovules as well as brown and shrivelled seeds that seemed to have arrested their development in a later stage of maturation. The proportion of *ICU2/icu2-3* plants was in all cases higher than that of *ICU2/icu2-2*, further indicating that the deleterious effects of *icu2-2* are stronger than those of *icu2-3*. Similar conclusions were reached from the analysis of reciprocal *icu2-1/icu2-1* ×

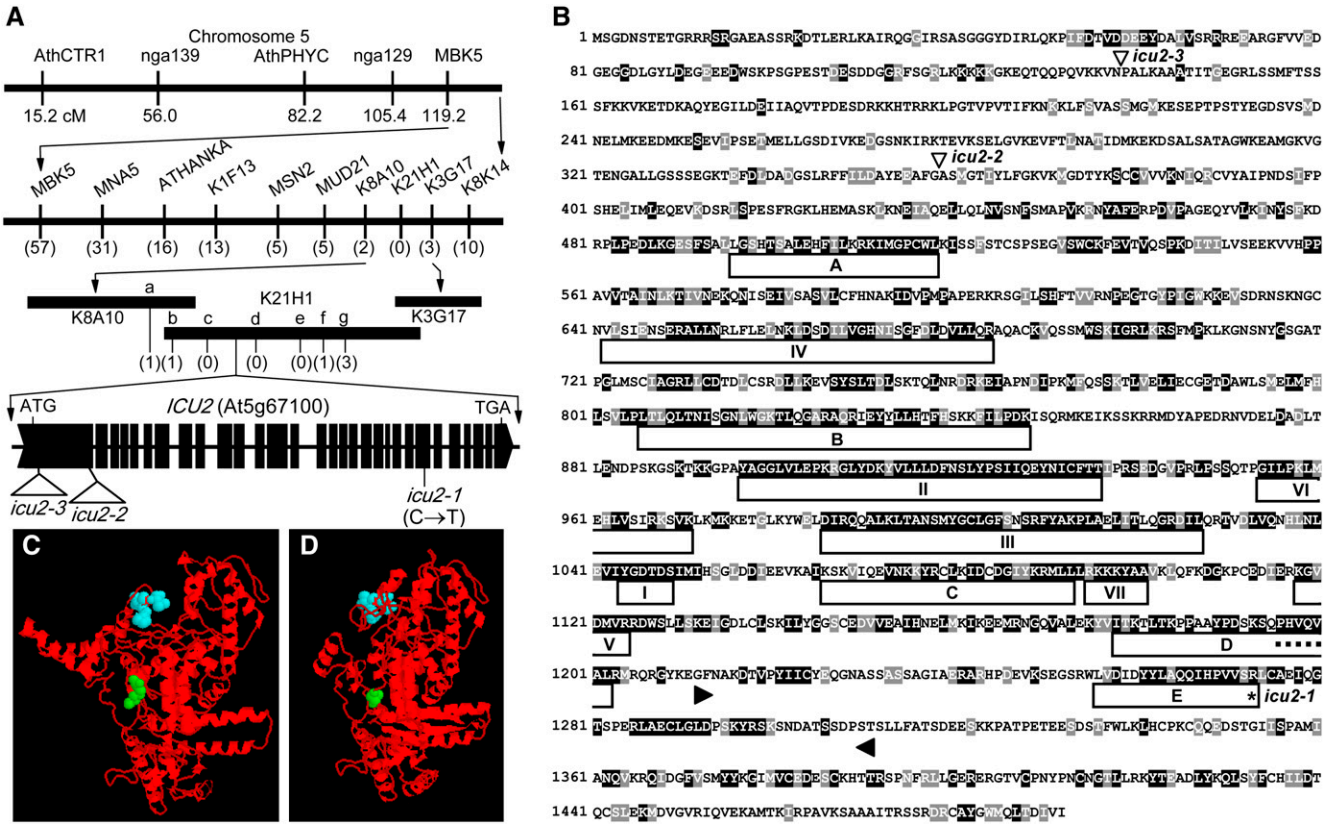

Figure 2. Positional Cloning and Structural Analysis of the *ICU2* Gene.

(A) Map-based strategy followed for the cloning of the *icu2-1* mutation. A mapping population of 1000 F2 plants, derived from *icu2-1*/*icu2-1* × Landsberg *erecta* (L*er*) and *icu2-1*/*icu2-1* × Columbia (Col-0) crosses (the *icu2-1* mutation was in an En-2 genetic background) was used to delimit *ICU2* to a region of 90 kb, which encompassed three overlapping transformation-competent artificial chromosome (Liu et al., 1999) clones. Several of the candidate genes were amplified and sequenced, allowing us to develop and use for further analyses seven previously unidentified single nucleotide polymorphism (SNP) markers (SNPk8a10-a and SNPk21h1-b to SNPk21h1-g; see Table 2), which were polymorphic between En-2 and either L*er* or Col-0. This reduced the candidate region to 50 kb, all whose putative transcription units (http://mips.gsf.de/proj/thal/db/index.html) were PCR amplified and sequenced. Only the At5g67100 gene, which encodes the catalytic subunit of DNA polymerase α, was found to carry a point mutation in the *icu2-1* mutant. The number of informative recombinants identified is indicated in parentheses. In the representation of the structure of the *ICU2* gene, exons are indicated by boxes, introns by lines between boxes, and T-DNA (*icu2-2*) and *Ds* (*icu2-3*) insertions by triangles. cM, centimorgan.

(B) Predicted amino acid sequence of the catalytic subunit of DNA polymerase α in *Arabidopsis*. The domains named as I to VII in Wang et al. (1989) and A to E in Miyazawa et al. (1993) are boxed. The region assumed to interact with primase is bordered by arrowheads (Biswas et al., 2003). The putative HP1 binding pentamere (MIR domain) is indicated by a dotted line, the position of the *icu2-1* mutation by an asterisk, and the *icu2-2* (T-DNA) and *icu2-3* (*Ds*) insertions by triangles. Residues shaded in black and gray indicate the identities and similarities, respectively, found after the alignment of the sequence of the *Arabidopsis* DNA polymerase α catalytic subunit (GI 15240200) with those of *Homo sapiens* (8393995), *Mus musculus* (6679409), *D. melanogaster* (217344), *Caenorhabditis elegans* (32565317), *O. sativa* (6015010), *S. pombe* (6018683), and *Neurospora crassa* (32416196). The sequences were aligned using the ClustalX 1.5b program (Thompson et al., 1997) and shaded with BOX SHADE 3.21 (http://www.ch.embnet.org/software/BOX_form.html). The gaps generated by the alignment have been removed.

(C) and **(D)** Models for the three-dimensional structure of the protein products of the En-2 wild-type **(C)** and *icu2-1* **(D)** alleles of the *ICU2* gene. The residue affected by the mutation is in green, and the HP1 binding domain is in blue. The three-dimensional models were obtained using the 3D-JIGSAW (Bates et al., 2001; http://www.bmm.icnet.uk/~3djigsaw/) and RasMol 2.7 (Sayle and Milner-White, 1995; http://www.umass.edu/microbio/rasmol/) programs.

ICU2/*icu2-2* and *icu2-1*/*icu2-1* × *ICU2*/*icu2-3* crosses. Although gametogenesis seemed to be affected also by the weak *icu2-1* allele, the aborted or unfertilized ovules found in the siliques of nonmanipulated, naturally selfed *icu2-1*/*icu2-1* plants were absent from *icu2-1*/*icu2-1* siliques pollinated by hand with *icu2-1* pollen. This suggests that the early lethality observed in *icu2-1*/*icu2-1* plants is due to insufficient pollen quantity rather than poor pollen quality. Taken together, these results indicate that the *icu2-2* and *icu2-3* alleles, but not *icu2-1*, affect both ovule and pollen formation.

The Phenotype of the *icu2-1* Mutant Is Largely Due to the Derepression of *AG* and *FT*

Given that the early flowering phenotype of the *tfl2* mutants is suppressed (Kotake et al., 2003) by mutations at the flowering

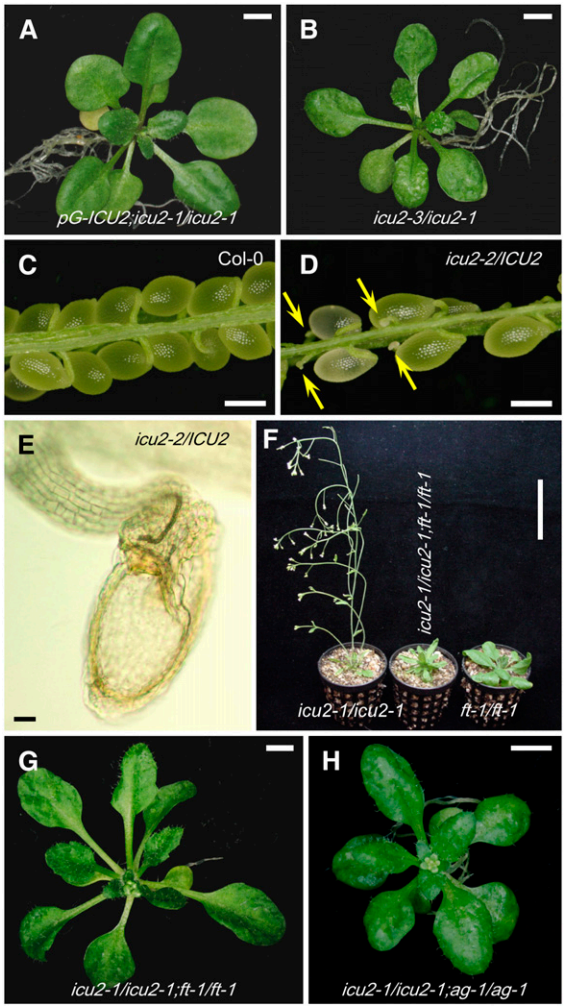

Figure 3. Other Phenotypic Traits of *icu2* Alleles and Suppression of Some of Them by *ag* and *ft* Mutations.

(A) and **(B)** Rosettes from a phenotypically wild-type transgenic line carrying the *pG-ICU2* wild-type transgene in an *icu2-1/icu2-1* background, demonstrating the phenotypic rescue of *icu2-1* by the wild-type allele of At5g67100 **(A)** and an *icu2-3/icu2-1* heterozygote **(B)**, which is indistinguishable to the *icu2-1/icu2-1* homozygotes.

(C) to **(E)** Dissected siliques from selfed Col-0 **(C)** and heterozygous *icu2-2/ICU2* (**[D]**; in a Col-0 genetic background) plants. Arrows in **(D)** indicate abnormal seeds that are likely to be aborted or unfertilized ovules. One of the latter is magnified in **(E)** as seen with Nomarski optics and did not display any embryonic structure, which was clearly visible in the morphologically normal seeds.

(F) to **(H)** Suppression of some of the phenotypic traits of the *icu2-1* mutation by loss-of-function mutations in *FT* and *AG*.

(F) and **(G)** Early flowering is suppressed in *icu2-1/icu2-1;ft-1/ft-1*.

(H) Leaf incurvature is suppressed in *icu2-1/icu2-1;ag-1/ag-1* double mutant plants.

Images were taken 21 (**[A]**, **[B]**, **[G]**, and **[H]**), 40 (**[C]** to **[E]**), and 35 **(F)** d after sowing. Bars = 2 mm in **(A)**, **(B)**, **(G)**, and **(H)**, 1 mm in **(C)** and **(D)**, 0.1 mm in **(E)**, and 5 cm in **(F)**.

promoter gene *FLOWERING LOCUS T* (*FT*; Kobayashi et al., 1999), and due to the resemblance between the phenotypes of *tfl2-2*, *icu2-1*, and *clf-2*, we crossed the *ft-1* mutant to either *icu2-1* or *clf-2*. Given that the double mutants displayed the leaf morphology of their *icu2-1* or *clf-2* parentals and late flowering, such as that of *ft-1* (Figures 3F and 3G), we concluded that the early flowering of *icu2-1* requires FT. We already found that the severe loss-of-function *ag-1* mutation (Chen and Meyerowitz, 1999) suppressed the mutant phenotype of *icu2-1/icu2-1* leaves (Figure 3H), where not only *AG*, but also *APETALA1* (*AP1*; Mandel et al., 1992), *AP3* (Jack et al., 1992), and *PISTILLATA* (*PI*; Bowman et al., 1989) were ectopically derepressed (Serrano-Cartagena et al., 2000). We obtained in this work double mutant combinations of *icu2-1* with the strong loss-of-function *ap1-1* (Bowman et al., 1993), *ap3-4* (Jack et al., 1992; Irish and Yamamoto, 1995), and *pi-1* (Bowman et al., 1991) mutations and found that both leaf morphology and flowering time of all the double mutants were similar to those of the *icu2-1* single mutant. These results indicate that both *AG* and *FT* are epistatic to *ICU2* and that their derepressions (see below) cause leaf incurvature and early flowering, respectively, in the *icu2-1* mutant; the results also show that *FT* is repressed not only by *TFL2* but also by *CLF* and *ICU2*.

ICU2 Genetically Interacts with *CLF*, *TFL2*, *EMF2*, *FAS1*, and *FAS2*

Ectopic expression of *AG* and other MADS box genes is known to be caused by loss of function of *TFL2*, *CLF*, or *EMF2*, among others (reviewed in Schubert et al., 2005). The mutants affected in these genes share several phenotypic traits with *icu2-1*, including leaf curvature and early flowering. Therefore, we decided to analyze the genetic interactions between *icu2*, *tfl2*, *clf*, and *emf2*. We obtained double mutants involving *icu2-1* (Figure 4B) and the null *clf-2* (Goodrich et al., 1997) and *tfl2-2* (Kotake et al., 2003) mutations (Figures 4C and 4D). The phenotypes of the *icu2-1 clf-2*, *icu2-1 tfl2-2*, and *clf-2 tfl2-2* double mutants (Figures 4E to 4G) were very similar and much more severe than those of either parental, displaying strongly incurved and narrow leaves arranged in an extremely small rosette. These synergistic genetic interactions suggested that the *ICU2*, *CLF*, and *TFL2* genes are functionally related.

The *emf2-5* mutant carries a weak hypomorphic allele of the *EMF2* gene (Yang et al., 1995; Chen et al., 1997), is extremely early flowering, and develops a tiny rosette composed of small, narrow, and involute leaves (Yoshida et al., 2001; Figure 4H). Its phenotype is similar to those of the *icu2-1 clf-2*, *icu2-1 tfl2-2*, and *clf-2 tfl2-2* double mutants. We found *emf2-5* to be epistatic to *icu2-1*, as deduced from a comparison of the *icu2-1/icu2-1;emf2-5/emf2-5* plants (Figure 4I) with their *ICU2/-;emf2-5/emf2-5* siblings, which were phenotypically indistinguishable in the F2 progeny (427 plants) of an *emf2-5/emf2-5* × *icu2-1/icu2-1* cross. Taken together with the previously described epistasis of *emf2* to *clf* (Chanvivattana et al., 2004), our results suggested a functional relationship among *ICU2*, *CLF*, *TFL2*, and *EMF2* genes.

We also crossed the *icu2-1* mutant to viable mutants defective in Chromatin Assembling Factor-1 (CAF-1) function, which is required for histone deposition in *Arabidopsis* (Schönrock et al., 2006). CAF-1 is a heterotrimeric complex that includes the CAC1,

Table 1. Transmission of *icu2* Alleles

Crosses (Female × Male)	Seed Phenotype as Shown in Opened Siliques			Phenotypes of Plants Grown on									
				Antibiotic-Supplemented Medium							Nonsupplemented Medium		
	Aborted or Unfertilized Ovules	Aborted Seeds	Mature Seeds	Ungerminated Seeds	Sul^r Wild Type	Sul^r Icu2	Sul^s	Kan^r Wild Type	Kan^r Icu2	Kan^s	Ungerminated Seeds	Wild Type	Icu2
ICU2/ICU2 × *ICU2/ICU2*	2	0	726								0	175	
icu2-1/icu2-1 × *icu2-1/icu2-1*	102	0	327								0		175
ICU2/icu2-2 × *ICU2/icu2-2*	413	0	424	0	84		467						
ICU2/ICU2 × *ICU2/icu2-2*	63	0	118	9	6		38						
ICU2/icu2-2 × *ICU2/ICU2*	99	0	90	22	11		126						
ICU2/icu2-3 × *ICU2/icu2-3*	160	45	389	0				275		273			
ICU2/ICU2 × *ICU2/icu2-3*	40	9	62	7				27		30			
ICU2/icu2-3 × *ICU2/ICU2*	17	4	100	8				92		104			
icu2-1/icu2-1 × *ICU2/icu2-2*	41	2	15	8	0	0	2				9	22	0
ICU2/icu2-2 × *icu2-1/icu2-1*	106	0	65	26	0	0	84				14	71	0
icu2-1/icu2-1 × *ICU2/icu2-3*	24	11	36	10				0	9	12	0	10	10
ICU2/icu2-3 × *icu2-1/icu2-1*	54	18	175	1				0	44	50	3	68	53
icu2-1/icu2-3 × *icu2-1/icu2-3*	99	100	172	7				0	87	46	2	0	36
ICU2/icu2-2 × *ICU2/icu2-3*	28	1	5	2	3		9	4		12			

Sul^r, sulfadiazine resistant; Sul^s, sulfadiazine sensitive; Kan^r, kanamycin resistant; Kan^s, kanamycin sensitive; Icu2, mutant morphology indistinguishable from that of *icu2-1/icu2-1* plants.

CAC2, and CAC3 proteins in yeast, p150, p60, and p48 in mammals, and FAS1, FAS2, and MSI1 in plants, loss of function of which results in transcription of some silenced genes. Mammalian CAF-1 is necessary for coupling chromatin assembly with DNA replication (Hoek and Stillman, 2003), and its p150 subunit is known to interact with HP1 (Murzina et al., 1999; Quivy et al., 2004). The *fas1* and *fas2* mutants of *Arabidopsis* are characterized by fasciated and flat stems, disrupted phyllotaxy, altered floral organ structure and number, leaf serration, and inhibition of root elongation (Leyser and Furner, 1992; Figures 5B and 5E). We crossed *icu2-1* to the *fas* mutants and found that the *icu2-1 fas1-1* double mutant displayed a synergistic phenotype consisting of small, narrow, and involute leaves (Figures 5C, 5D, and 5F), similar to those of the *icu2-1 clf-2* and *icu2-1 tfl2-2* double mutants obtained in this work. In addition, the *icu2-1 fas1-1* floral organs had much more severe alterations than those of either parental (Figure 5F), displaying disrupted phyllotaxy and strongly curly siliques, which only contained aborted or unfertilized ovules. In addition, we performed an *icu2-1/icu2-1* × *fas2-1/fas2-1* cross, finding in its F2 progeny no *icu2-1/icu2-1;fas2-1/fas2-1* plants, as well as a reduced frequency of the *icu2-1/icu2-1;FAS2/fas2-1* and *ICU2/icu2-1;fas2-1/fas2-1* genotypes (expected, 2/15 each; observed, 1/100 each), which were phenotypically indistinguishable to their *icu2-1/icu2-1;FAS2/FAS2* and *ICU2/ICU2;fas2-1/fas2-1* siblings, respectively.

A Number of Genes Encoding Transcription Factors Are Upregulated in the *icu2-1* Mutant

When *ICU2* transcript levels were analyzed in assorted tissues of the wild-type En-2 by means of quantitative RT-PCR (QRT-PCR; Figure 6A), we found ~10-fold more expression in shoot apices (where meristematic cells are more abundant) than in roots, flower buds, open flowers, and siliques, which, in turn, displayed 10-fold more expression than the whole rosettes that were used as a reference. The lowest levels of *ICU2* activity were found in leaves and stems. The *icu2-1* point mutation did not significantly change the transcriptional activity of the *ICU2* gene in rosettes or in shoot apices (Figure 6B). The same conclusion can also be reached by examining the expression profiles of *ICU2* obtained from Genevestigator (http://www.genevestigator.ethz.ch; Zimmermann et al., 2004).

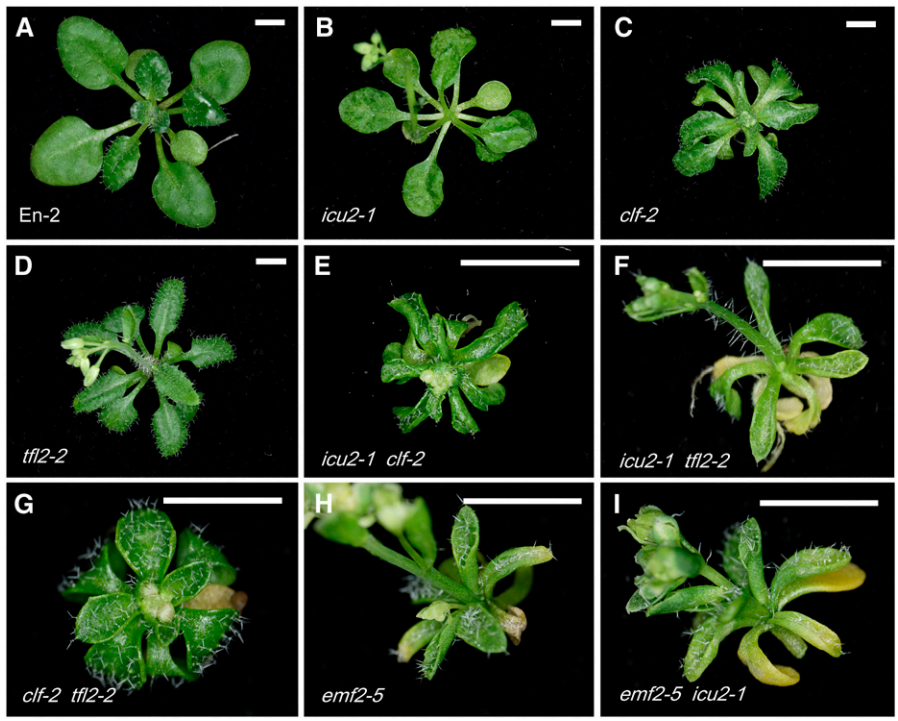

Figure 4. Genetic Interactions between Mutations Affecting *ICU2* and Genes Involved in Chromatin-Mediated Cellular Memory.

Rosettes are shown for the wild-type En-2 **(A)** and single (**[B]** to **[D]** and **[H]**) and double mutants (**[E]** to **[G]** and **[I]**). All plants shown were homozygous for the indicated mutations. Images were taken 21 d after sowing. Bars = 2 mm.

Using a nonquantitative method, we have already demonstrated the ectopic expression of the *AG*, *AP1*, *AP3*, and *PI* genes in the leaves of the *icu2-1* mutant (Serrano-Cartagena et al., 2000). In this work, we used QRT-PCR to analyze the expression of these genes and of other genes, which included several members of the MADS box family (*SEPALLATA3* [*SEP3*; Pelaz et al., 2000], *CAULIFLOWER* [*CAL*; Kempin et al., 1995], *FRUITFULL* [*FUL*; Gu et al., 1998], *FLC* [Michaels and Amasino, 1999], and *SUPRESSOR OF OVEREXPRESSION OF CONSTANS1* [*SOC1*; Lee et al., 2000]), as well as meristem identity and flowering time genes (*FT*, *LEAFY* [*LFY*; Weigel et al., 1992], and *WUSCHEL* [*WUS*; Laux et al., 1996]). We found strongly upregulated the *AG*, *AP1*, *AP3*, *PI*, *SEP3*, *CAL*, *FUL*, *SOC1*, and *FT* genes both in excised leaves and whole rosettes of the *icu2-1* mutant (Figures 5C and 5D), as well as *LFY* and, particularly, *WUS* only in whole rosettes (Figure 5D). To ascertain whether derepression of the *AG*, *AP1*, *AP3*, or *PI* floral organ identity genes might in turn be the cause of the derepression of the rest of the studied genes, we obtained the *icu2-1 ag-1*, *icu2-1 ap1-1*, *icu2-1 ap3-4*, and *icu2-1 pi-1* double mutants and found no significant differences between their QRT-PCR analyses and those of the *icu2-1* single mutant. These results indicated that derepression of *SEP3*, *SEP1*, *SEP2*, *CAL*, *FUL*, *SOC1*, *FT*, *LFY*, and *WUS* is not an indirect consequence of *AG*, *AP1*, *AP3*, or *PI* deregulation in the *icu2-1* mutant.

Given the pivotal contribution of *AG* and *FT* derepression to the phenotype of the *icu2-1*, *clf-2*, and *tfl2-2* mutants, and due to the important role of *SEP3* and *WUS* in flower organogenesis and meristem function, respectively, we decided to quantify the expression of these four genes in the *icu2-1*, *clf-2*, *tfl2-2*, and *emf2-5* single mutants as well as in the *icu2-1 tfl2-2*, *icu2-1 clf-2*, and *clf-2 tfl2-2* double mutants. We found the *AG*, *SEP3*, *FT*, and *WUS* genes to be upregulated (Figure 5E). *AG* and *FT* transcript levels were similar in the double mutants and the *emf2-5* single mutant and clearly higher than those observed in the *icu2-1*, *clf-2*, and *tfl2-2* single mutants. The highest *WUS* transcript levels were observed in the *icu2-1* single mutant and the *icu2-1 tfl2-2* and *icu2-1 clf-2* double mutants, suggesting a role for *ICU2* in the repression of this meristematic gene.

The *AG* Locus Is Enriched in the H3ac Active Mark in the *icu2-1* Mutant

The genetic interactions among *ICU2*, *CLF*, *TFL2*, *EMF2*, *FAS1*, and *FAS2* described here and the derepression of regulatory genes that we observed in the *icu2-1* mutant suggested a role for *ICU2* in epigenetic inheritance and plant chromatin packaging. In addition, it is known that expression of *AG* and *STM*, which are direct *CLF* targets, depends on their histone methylation pattern (Schubert et al., 2006). This prompted us to perform a chromatin immunoprecipitation (ChIP) analysis to test whether the *icu2-1* mutation affects epigenetic marks in *AG*, which is derepressed in the *icu2-1* mutant.

We tested the dimethylation of Lys-9 of histone H3 (H3K9me2), which in *Arabidopsis* is localized within silent heterochromatin (Lindroth et al., 2004), and the trimethylaltion of Lys-27 of H3 (H3K27me3), which is preferentially associated with open

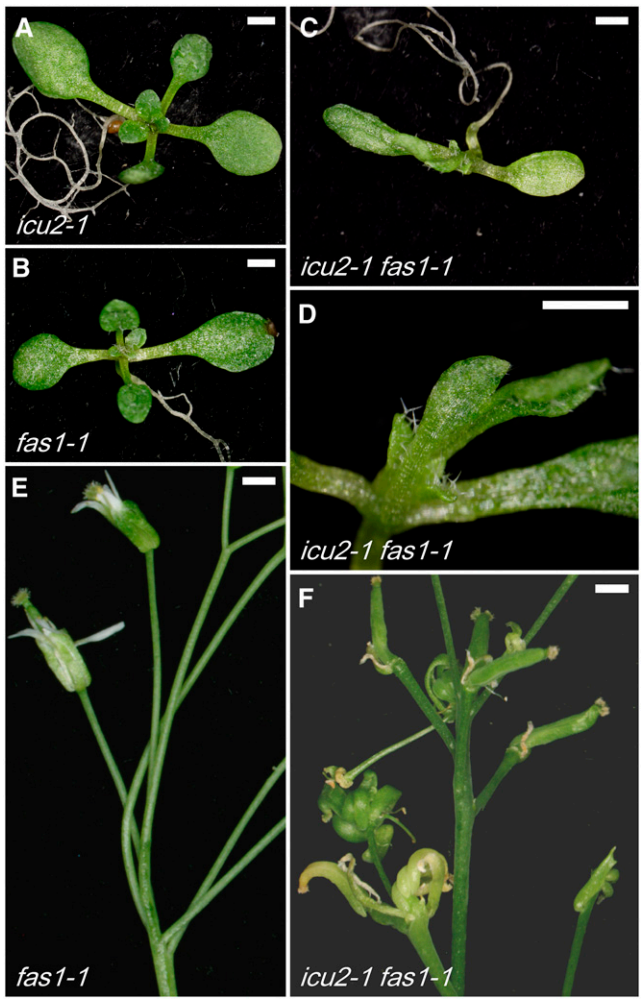

Figure 5. Genetic Interactions between Mutations Affecting *ICU2* and *FAS1*.

Plants are shown for single (**[A]**, **[B]**, and **[E]**) and double (**[C]**, **[D]**, and **[F]**) mutants. A magnification of the lateral view of **(C)** is highlighted in **(D)**. All plants shown were homozygous for the indicated mutations, and all the mutants are in an En-2 background. Images were taken 10 d (**[A]** to **[D]**) and 2 months (**[E]** and **[F]**) after sowing. Bars = 1 mm.

euchromatin regions (reviewed in Henikoff, 2005). These two epigenetic marks were not significantly changed in the promoter and second intron of the *AG* gene (Figure 7). We also tested H3 acetylation and found a noticeable enrichment of H3ac in the *AG* promoter in the *icu2-1* mutant (Figure 7). To determine whether or not these histone modifications were associated with changes in DNA methylation, we analyzed by bisulfite genomic sequencing the *AG* promoter and found that cytosine methylation was not significantly different in the *icu2-1* mutant (0.38%; 15 clones sequenced) and the En-2 wild type (1.32%; 10 clones).

ICU2 Interacts with TFL2 in Vitro

To analyze the physical interaction between ICU2 and TFL2, we expressed in bacteria TFL2 fused to the glutathione *S*-transferase (GST) protein. Both GST and GST-TFL2 proteins bound to sepharose beads were incubated with the carboxylic half of the wild-type ICU2 protein (ICU2-ct) and that of its mutated version (ICU2-1-ct), which had been translated in vitro in the presence of radiolabeled Met. GST-TFL2 interacted with the full-length ICU2-ct but not with the full-length ICU2-1-ct protein (Figure 8). Interestingly, a smaller subproduct of the synthesis of the ICU2-1-ct protein, which according to the molecular weight deducted from its migration in the gel contains the HP1 binding domain but not the amino acid changed by the *icu2-1* mutation, was able to interact with GST-TFL2. This result indicated that the wild-type ICU2 protein interacts with TFL2 and suggested that the *icu2-1* mutation disturbs somehow such interaction.

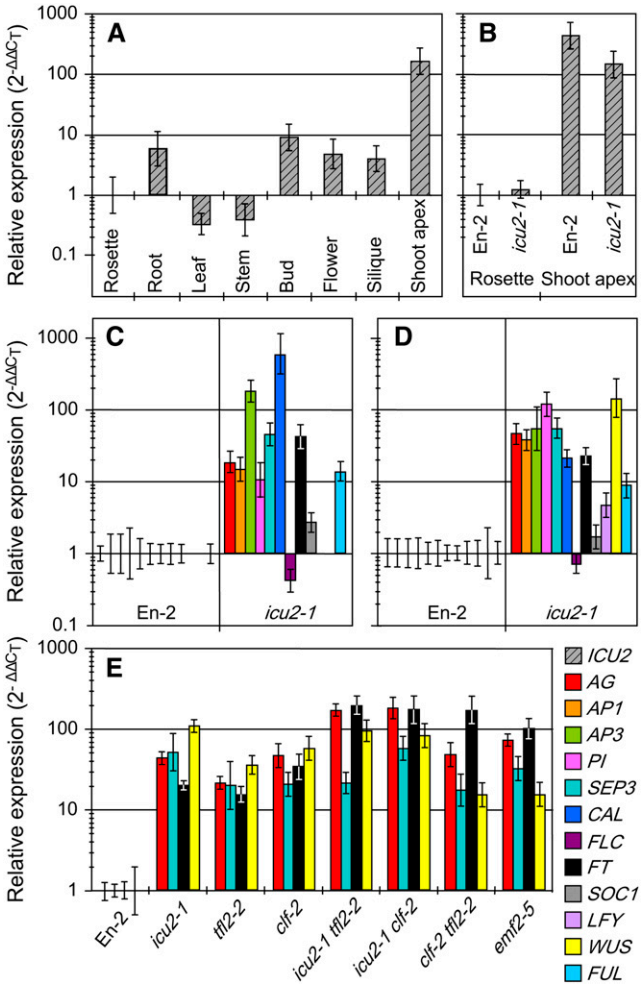

Figure 6. QRT-PCR Analyses.

Quantifications are shown for the transcript levels of *ICU2* (**[A]** and **[B]**) in assorted tissues of the wild-type En-2 **(A)** and rosettes and shoot apices of En-2 and the *icu2-1* mutant **(B)**, as well as for those of the indicated genes in leaves **(C)** or whole rosettes (**[D]** and **[E]**) of the *icu2-1* mutant (**[C]** and **[D]**) and some other single and double mutants **(E)**. All plants were homozygous for the mutations indicated. Plant material was collected 21 d after sowing, with the roots being removed before the extraction of rosette RNA. All data were referred (using the $2^{-\Delta\Delta C_T}$ method) to those obtained for the En-2 wild type, to which a value of 1 was given.

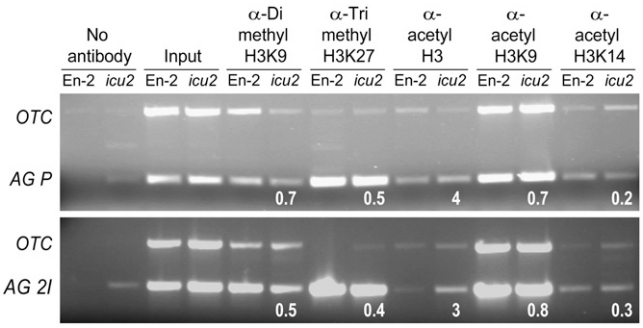

Figure 7. ChIP Assay.

The histone methylation and acetylation patterns of the promoter (*AG P*) and second intron (*AG 2I*) of *AG* in the En-2 wild type and the *icu2-1* mutant (lanes headed as *icu2*) were tested. ChIP duplex PCR was used to amplify the *ORNITHINE TRANSCARBAMILASE* (*OTC*) gene and regions of the *AG* gene. Numbers below gel lanes indicate the ratio of the intensity of *AG* products compared with that of *OTC* products after normalization with input product intensity (Schubert et al., 2006).

The Spatial Expression Patterns of *AG* and TFL2 Are Patchy in the *icu2-1* Mutant

To visualize the spatial expression pattern of *AG* in *icu2-1/icu2-1* leaves, a transgenic line carrying the *pAG-I:β-glucuronidase* (*GUS*) reporter construct (Sieburth and Meyerowitz, 1997) was crossed to *icu2-1/icu2-1* and En-2 plants. No GUS staining was observed in the leaves of the F2 plants carrying the transgene in a wild-type background (Figure 9A), whereas patches of GUS-stained cells were frequent in the *pAG-I:GUS;icu2-1/icu2-1* leaves (Figures 9B to 9D). This patchy ectopic *AG* expression was displayed by mesophyll, epidermal, and vascular cells of *icu2-1/icu2-1* leaves. The expression of *pAG-I:GUS* was also studied in a *tfl2-2/tfl2-2* mutant background, with GUS staining only being found in vascular tissues.

The spatial distribution of the TFL2 protein was studied in En-2 and *icu2-1/icu2-1* leaves using the *gTFL2:green fluorescent protein* (*GFP*) transgene (Kotake et al., 2003), which contains the whole coding sequence and the promoter of *TFL2*. All wild-type leaf cells displayed a nuclear GFP signal (Figure 9E), as reported previously (Gaudin et al., 2001; Kotake et al., 2003). A similar GFP subcellular localization was observed in many transgenic *icu2-1/icu2-1* leaves (Figure 9F), which displayed in addition patches of cells in which the signal was both nuclear and cytoplasmic (Figure 9G) and extremely high (Figure 9H). Although the size and distribution of the patches showing ectopic *AG* expression were very similar to those showing perturbation of TFL2 subcellular distribution, we have no proof of their colocalization.

DISCUSSION

Mutant Alleles of *ICU2*, a Plant Gene Encoding a DNA Polymerase α Subunit

Five eukaryotic DNA polymerases have been classically described (α, β, δ, ε, and γ; Kornberg and Baker, 1991), to which at least another 10 have been added in the last years (Hubscher et al., 2002). The β and ε polymerases have been associated with repair and the α and δ with replication, all of them in the nucleus, whereas the γ polymerase is required for mitochondrial DNA replication. The *Arabidopsis* gene encoding DNA polymerase ε is the only plant DNA polymerase gene that has been studied at a mutational level so far, with all its described mutant alleles causing gametic or embryonic lethality (Jenik et al., 2005; Ronceret et al., 2005).

We positionally cloned *ICU2* (At5g67100), a single-copy gene encoding the putative catalytic subunit of DNA polymerase α, and identified and characterized three *icu2* mutant alleles. DNA polymerase α is an essential piece in the cell cycle, where it is required for the initiation of replication; in all eukaryotes, it consists of a catalytic core, two primases, and the so-called B-subunit (of 170, 50, 60 and 70 to 75 kD, respectively; Uchiyama and Wang, 2004). These proteins are encoded in *Arabidopsis* by the At5g67100, At5g41880, At1g67320, and At1g67630 genes, respectively. Consistent with its important role in the initiation of DNA replication, transcription of the gene encoding the DNA polymerase α catalytic subunit is known to be cell cycle regulated in *D. melanogaster*, *S. pombe*, and human cells (Wahl et al., 1988; Hirose et al., 1991; Bouvier et al., 1992). In plants, its activity has been seen to peak before the S phase in rice (*Oryza sativa*) and maize (*Zea mays*; Yokoi et al., 1997; Gómez Roig and Vázquez-Ramos, 2003). As expected, the *ICU2* promoter included the consensus sequence characterizing cell cycle–regulated genes, and its expression was higher in the tissues showing higher cell division rates, such as the shoot apex.

As expected from the essential role played by replication machinery elements, including DNA polymerase α, the strong *icu2-2* and *icu2-3* insertional alleles caused fully penetrant zygotic lethality when homozygous and incompletely penetrant gametophytic lethality, probably because of loss of DNA polymerase activity. The early lethality of these alleles is likely to be due to their inability to contribute to the initiation of replication in

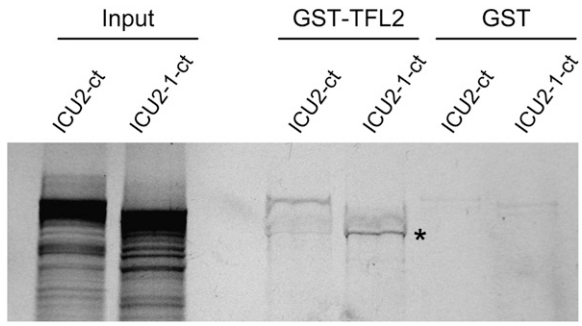

Figure 8. GST Pull-Down Assay Demonstrating Direct Interaction between the TFL2 and ICU2 Proteins.

The carboxylic half of the wild-type ICU2 protein (ICU2-ct) and that of its mutated version (ICU2-1-ct) were translated in vitro in the presence of ^{35}S-Met. GST-TFL2, but not GST, was able to interact with the full-length ICU2-ct as well as with a truncated ICU2-1-ct protein (indicated by an asterisk). GST-TFL2 did not interact with the full-length ICU2-1-ct. The input lane shows the signal from 10% of the amount of in vitro–translated ICU2-ct and ICU2-1-ct proteins present in each of the remaining samples.

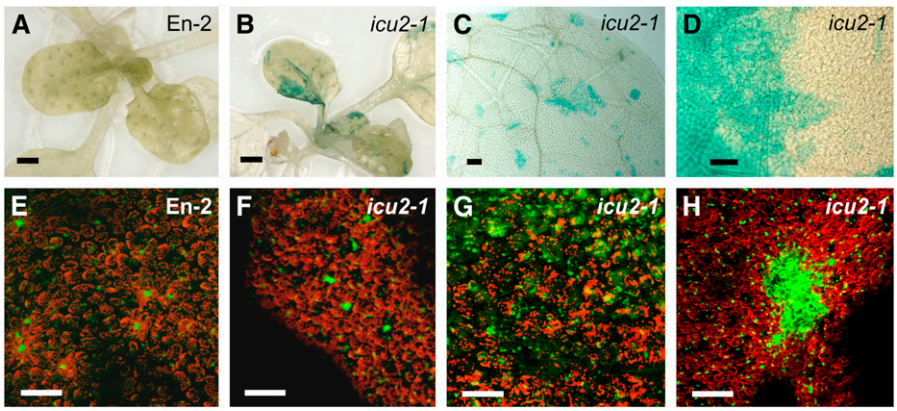

Figure 9. *AG* and TFL2 Spatial Expression Patterns in the *icu2-1* Mutant.

(A) to **(D)** GUS staining of leaves of transgenic plants carrying the *pAG-I:GUS* construct in En-2 **(A)** and *icu2-1*/*icu2-1* (**[B]** to **[D]**) backgrounds.
(E) to **(H)** Confocal micrographs of leaves from transgenic plants carrying the *gTFL2:GFP* construct in En-2 **(E)** and *icu2-1*/*icu2-1* (**[F]** to **[H]**) backgrounds. All plants shown were homozygous for the indicated mutations. Images were taken 21 d after sowing. Bars = 1 mm in **(A)** and **(B)** and 100 μm in **(C)** to **(H)**.

gametogenesis or early postfertilization. Although no phenotypic evidence of perturbation in DNA replication was observed in the *icu2-1* mutant, we cannot exclude that it also lacks some degree of polymerase α activity. The phenotypic effects of the *icu2-2* allele were the most severe, and the lethality of the *icu2-1*/*icu2-2* genotype versus the viability of *icu2-1*/*icu2-3* suggested that *icu2-2* might not only be an extreme loss-of-function allele but also antimorphic. Although our *icu2* alleles might shed light on plant DNA replication, further molecular research on their effects on the polymerase activity of ICU2 will be needed, which is beyond the scope of this work.

Genetic and Physical Interactions between ICU2 and TFL2

Like many other DNA polymerases, the structure of the catalytic DNA polymerase α subunit has been compared with a right hand and divided into three canonical domains termed palm, fingers, and thumb (Wang et al., 1997; Rothwell and Waksman, 2005). In *Saccharomyces cerevisiae*, single mutations in the palm region affect replication fidelity and genomic stability (Limsirichaikul et al., 2003; Niimi et al., 2004), whereas those damaging the fingers reduce processability or the replication rate (Ogawa et al., 2003). In *S. pombe*, only a few weak alleles of *Swi7*, the gene encoding DNA polymerase α, have been isolated, and null alleles are recessive lethal (Singh and Klar, 1993). The *swi7-H4* allele carries a mutation in the conserved box VI and uncouples mitosis and DNA synthesis (Murakami and Okayama, 1995). The *swi7-1* allele causes a Gly-to-Glu change in position 1116 of the thumb domain (12 residues upstream to the MIR domain) and perturbs mating-type switching. These results suggest a role for DNA replication in the organization of cellular differentiation programs (Singh and Klar, 1993). The *icu2-1* mutation described here affects the thumb, changing the three-dimensional structure of the ICU2 protein, which probably affects accessibility to its MIR domain.

Both the presence of a MIR domain in ICU2 and the genetic interaction described here between the *icu2-1* and *tfl2-2* mutations pointed to the physical interaction of ICU2 and TFL2. In addition, a computer-based prediction of protein structure suggested that the *icu2-1* mutation collapses the ICU2 thumb, which in turn could reduce or abolish the access of TFL2 to the MIR domain. We confirmed this genetic evidence by demonstrating that TFL2 binds to wild-type ICU2, a protein–protein interaction that is likely to be impaired by the amino acid substitution caused by the *icu2-1* mutation.

We found in the *icu2-1* mutant an abnormal subcellular distribution of TFL2, which was restricted to the nucleus in most leaf cells, but appeared in both the nucleus and the cytoplasm in other cells, which were often clustered. This suggested that reduced or abolished interaction between ICU2 and TFL2 perturbs the nucleocytoplasmic distribution of TFL2. However, we cannot rule out the possibility of position effect variegation, due to the characteristics of the genomic region flanking the *gTFL2:GFP* transgene, as the cause of the patchy redistribution and increase of the TFL2:GFP protein.

A Link between DNA Replication and Chromatin-Mediated Gene Repression in the Plant Kingdom

Several lines of evidence indicate a link between the DNA replication machinery and cellular memory (McNairn and Gilbert, 2003; Vermaak et al., 2003; Craig, 2004). On the one hand, mutations in the origin recognition complexes affect the repression state of different genes in yeast and perturb position effect variegation in *D. melanogaster* (Pak et al., 1997). On the other hand, some chromatin-associated proteins, such as HP1 or those of the CAF complexes, are known to physically interact with elements of the replication machinery, such as proliferating cell nuclear antigen (Zhang et al., 2000; Ehrenhofer-Murray, 2004; Sarraf and Stancheva, 2004). In addition, the DNA polymerase α Swi7 binds to the HP1 homolog Swi6 in *S. pombe*, and the *swi7-1* and *swi7-H4* mutants, which lack such interaction, display deregulation of the mating-type region and an abnormal

Table 2. Primer Sets Used in This Work

Purpose	Template	Oligonucleotide Sequences (5′→3′)		PCR Product Size (bp) and Polymorphisms[a]
		Forward Primer	Reverse Primer	
Linkage analysis	SNPk8a10-a	TTTTGCTCTTCTCGTCGGTGAA	TCAGTTAAAACCTACCTTAGACC	961; A324 (Col-0), G (En-2, L*er*)
	SNPk21h1-b	AGAAATACTATGCTGCATTGTCC	TTCTTCTCCATAAATTCACCAAAC	714; G145 (Col-0, En-2), C (L*er*)
	SNPk21h1-c	ACTTCAGTGCGAAGCACCCC	AGAACTTTATCAGACAACTCTCC	253 (Col-0, En-2), 246 (L*er*)
	SNPk21h1-d	TTTGAATGGAAGAGTTAAATGGTG	ATGATTACGTAAAATCACGGAATG	686; G460 (Col-0), C (En-2), A (L*er*)
	SNPk21h1-e	CAGCGTCTTTCCCATTACACTT	ATACTCCCATCTACATCCTACAT	1739; G205 (Col-0, En-2), C (L*er*); C812 (Col-0, En-2), G (L*er*)
	SNPk21h1-f	TTAACTTCCCTGAGCTTCTTCC	GGCGCTAATGATTCGTAGAAGC	406; T165 (Col-0, En-2), A (L*er*)
	SNPk21h1-g	TCTACGATTATCATCCTAATGGC	TCTCCTTTCTCTAAATTAACCCC	1331; A627 (Col-0, L*er*), C (En-2)
Genomic DNA amplification and cycle sequencing	*ICU2*	TTGCAGTTTAAGGATGGGAAGC	TGATTTCACCTCATCAGGATGC	871
	ICU2	ATAGAGAACAATGATTTTGGATATG	TAACTGGAACAGTACCTGGTAG	1053
	ICU2	AGGTTACTCCAGATGAGTCGG	ACTCGCCTTTAAGATCTTCTGG	1275
	ICU2	AAATCGTCTGTTTTCTTACATCTC	TGTGAAGGATCACAAACACAGC	1106
	ICU2	AAATTCAAAGAACGGCTGCAATG	AGTAAGCTGGAGAGTGAGAGG	1236
	ICU2	TCTTTTCTTTCAGATTGAATGTGG	TTAGACGATTATGTCAGAATTAGG	990
	ICU2	AGTATTGTATTGGTGACTGCTGC	ATTTTCTGCAAGAAAGGGTATGC	1089
	ICU2	TCTGTGCAGGGTAATGCTAGC	GTGCTTGCATGACTCGTCTTC	1024
	FAS1	ACTATGGTAGCTGTGAAGAGTG	TGAGCTGTTCTTCTGCATCATG	567
	FAS2	TATTTCTGGCTCAGTGGACAAC	GATCCATCAGGTGACCATGAC	502
Confirmation of insertions	*ICU2* and *Ds*	ATAGAGAACAATGATTTTGGATATG	ACCCGACCGGATCGTATCGGT[b]	854
	Ds and *ICU2*	GAAACGGTCGGGAAACTAGCTCTAC[c]	ACTCGCCTTTAAGATCTTCTGG	1405
	T-DNA	CCACACGTGGATCGATCCGTCG[d]	GAACCCTAATTCCCTTATCTGGG[e]	1181
	ICU2 and T-DNA	ATAGAGAACAATGATTTTGGATATG	ATATTGACCATCATACTCATTGC[f]	1590
Rescue	*ICU2*	ATAGCGGCCGCGTCTGAGCAAGTTTTTTTCTCT[g]	ATAGTCGACGCAGAAACTCATTCCCAATTCC[h]	9467
	pGreenII0179	TCTTCGCTATTACGCCAGCTG	GCGGATAACAATTTCACACAGG	332
QRT-PCR	*AG*	CCGATCCAAGAAGAATGAGCTCTT	CATTTTCAGCTATCTTTGCACGAA	110
	AP1	CGACGTCAATACAAACTGGTCGAT	CTTTAGGGCTCATTGCTTGCA	116
	AP3	CCCTAACACCACAACGAAGGAGAT	GTTTCCTCTTGGTTTCTTGCATTC	103
	CAL	CTCACGTTAATGCACAGACGAA	AGATCCTTGAGGCTCATTGGTT	126
	FLC	TTGAACTTGTGGATAGCAAGCTT	CGGTCTTCTTGGCTCTAGTCA	121
	FT	GAACAACCTTTGGCAATGAGATT	CACCCTGGTGCATACACTGTT	120
	FUL	CGACTCTTGCATGGAGAGGAT	CTTGAGCTTAGCATGTTCTAGAA	120
	ICU2	TGTTGAAGGAGGTCAGTTATTCT	CACAAGTGTTTTGGATGACTGAA	118
	LFY	CCCACCAAGGTGACGAACCA	ACAGTGAACGTAGTGTCGCATT	93
	OTC	TGAAGGGACAAAGGTTGTGTATGTT	CGCAGACAAAGTGGAATGGA	94
	PI	TTCAAATGCCTGAGCTCCAGTT	GCTAAGCATGAGAACCTTAGCA	83
	SEP3	TTAGCAGTTGAACTTAGTAGCCA	CCAAGATCTTCTCCCAACAGAT	100
	SOC1	GCCAGCTCCAATATGCAAGATA	CTTCATATTTCAAATGCTGCATATT	108
	WUS	TGGATCTATGGAACAAGACTGTT	GGCTTTGCTCTATCGAAGAAGT	113
Bisulfite sequencing[i]	*AG* promoter	AAGAAGAAGATTGATATTTGTTGTAAT	CTTATTAAAAACACCCCCAAATTAAA	281
	AG 2nd intron	AGATTTAGTTTTGTAGAATTAAGATTT	TCAAATATATAATATAATATAATTCATAAA	378
ChIP	*AG* promoter	GAAGAAGATCGATATTTGTTGTAAC	ATTAAGGACACCCCCAAATTGAG	276
	AG 3′ 2nd intron	TTCTTCTTCTCGTGCTCTGTTC	ATCTAAATCTTCAAGTACTTGTTAG	606
	AG 3′ 2nd intron	ATTCAGTTTTGTAGAACTAAGATTC	AATATATGATATGATATAATTCATGAG	373
	AG 3′ 2nd intron	TTACTTTCCTTTCTTATCTCTAGC	TACTAGTTTGAGTAATGTAGTTCG	485
	AG 5′ 2nd intron	CTCTCTCATTATGGGTACTGAG	TCAAATCGACCACTTGCACAGT	742
	AG 5′ 2nd intron	TGGAACGTTGTGATGTTACTCG	TCAAATCGACCACTTGCACAGT	478

[a] Polymorphisms are indicated by numbers that correspond to positions within the PCR amplification product, starting from the 5′ end of the forward primer.
[b,c] The sequences of Ds3-1[b] and Ds5-1[c] were obtained from the Arabidopsis Transposon Insertion Service.
[d,e,f] The sequences of Sulf-9525,[d] Sulf-10706,[e] and Lb-8409[f] were obtained from http://www.gabi-kat.de/General_Information/GABI-Kat-pAC161T-DNAmapPr.html.
[g,h] The 5′ tails of these oligonucleotides include restriction sites for *Not*I[g] and *Sal*I[h].
[i] We also used M13 forward and reverse standard primers.

chromosomal localization of Swi6. These latter observations indicate that some epigenetic marks are replicated simultaneously to DNA with the participation of the DNA replication complexes, at least in the fission yeast (Ahmed et al., 2001; Nakayama et al., 2001).

We hypothesize that the ICU2 DNA polymerase α plays a role in epigenetic inheritance in *Arabidopsis* by facilitating the interaction of TFL2 with histones, which results in propagation of epigenetic marks. In the *icu2-1* mutant, this reheterochromatinization polymerase-mediated process would be impaired, making unstable the repression of many genes. Given that the *icu2-1* mutation does not strongly affect viability or fertility, the interaction between ICU2 and TFL2 is probably not essential in *Arabidopsis* or not completely abolished in the *icu2-1* mutant, since the MIR

domain remains intact. In fact, in *S. pombe* mutants lacking Swi6–Swi7 interaction, DNA replication activity is almost normal and only the silencing of specific chromosomal regions is perturbed.

Chromatin-mediated gene repression is reduced by the *icu2-1* mutation but not completely abolished, as suggested by the morphological aberrations and gene deregulation levels of the *icu2-1* and *tfl2-2* mutants, which are weaker than those of the *icu2-1 tfl2-2* double mutant. The weak phenotype of the *tfl2-2* mutant may be due to redundancy with other genes of the chromodomain family. In the *icu2-1* mutant, chromatin-mediated cellular memory might fail for some genes in some cells and their progeny as a consequence of impaired TFL2–ICU2 interaction, which in turn would reduce or abolish TFL2–histone interaction, making the repression of TFL2-targeted genes unstable. This clonal behavior might explain the patchy pattern of epidermal cell size, *AG* ectopic expression, and TFL2 intracellular distribution found in the leaves of the *icu2-1* mutant.

The dose level of HP1 is known to affect position effect variegation in *D. melanogaster* (Ayyanathan et al., 2003), which is consistent with a dynamic structure of silent chromatin, as proposed in the site exposure model (Ahmad and Henikoff, 2002). In the *icu2-1* mutant, silent chromatin might lack epigenetic marks after replication longer than in the wild type, allowing misexpression of some genes. It is worth mentioning that ectopic expression of *AG* does not show a patchy pattern in the *tfl2-2* and *clf-2* mutants, in which it is uniform, which correlates with their not patchy morphological phenotype, consisting of leaf epidermal cells of reduced size (Larsson et al., 1998; Serrano-Cartagena et al., 2000). The patchy phenotype caused by the *icu2-1* mutation might be a useful trait for analyzing the mechanism by which the epigenetic marks are transmitted through mitosis after DNA replication.

Other Genetic Interactions of *ICU2*

We found the *emf2-5* mutation to be epistatic to *icu2-1*, *clf-2*, and *tfl2-2*. In addition, the morphological and molecular phenotypes of the *icu2-1 tfl2-2*, *icu2-1 clf-2*, and *tfl2-2 clf-2* double mutants are very similar to those of the *emf2-5* single mutant. Taken together, these results suggest that *EMF2* acts in the same pathway or plays a more general role than that of *ICU2*, *TFL2*, and *CLF*. It is worth noting that the phenotypes of weak *emf2* alleles are reminiscent of those of strong *clf* alleles (Chanvivattana et al., 2004), whereas those of the weak *clf-9* mutation and *icu2-1* are very similar. It seems that all these genes affect with different strengths the same biological process, which would be specifically related to the repression of *FT* and *AG*, among others.

The phenotype of the *clf-2* mutant is weaker than those of the *icu2-1 clf-2* and *tfl2 clf-2* double mutants, suggesting that other PcG proteins or complexes participate in the repression mechanism, as has been proposed based on the partial redundancy found between *CLF* and *SWINGER* (Chanvivattana et al., 2004). The synergistic phenotype of the *icu2-1/icu2-1;fas1-1/fas1-1* double mutants, together with the lethality of the *icu2-1/icu2-1;fas2-1/fas2-1* genotype, and the reduced frequency of the *icu2-1/icu2-1;FAS2/fas2-1* and *ICU2/icu2-1;fas2-1/fas2-1* plants clearly indicate a functional relationship between ICU2 and the CAF-1 histone deposition complex. These observations reinforce the notion of a functional relationship between chromatin remodeling machinery and the ICU2 DNA polymerase α.

Several Genes Derepressed by the *icu2-1* Mutation Are TFL2 Targets

Quantitative RT-PCR analyses in the *icu2-1* mutant allowed us to identify the upregulation of several closely related MADS box genes of the MIKC group (Parenicova et al., 2003) mainly responsible for floral organ identity, including *SEP1*, *SEP2*, *SEP3*, *AG*, *AP1*, *AP3*, *PI*, *CAL*, and *FUL*. In addition, the flowering promoter gene *FT* was found upregulated, while the flowering repressor gene *FLC* was downregulated. Derepression of these genes could be an indirect effect of the derepression of the direct targets of *ICU2*, as suggested by the demonstration of the regulation of *SEP3* and *FUL* by FT (Teper-Bamnolker and Samach, 2005).

Some of the genes that we found derepressed in the *icu2-1* mutant have been found upregulated in a microarray analysis performed on the *tfl2-3* mutant (*AG*, *AP3*, *FLC*, *PI*, and *SEP3*; Nakahigashi et al., 2005), and some are targeted by the TFL2 protein and enriched in the H3K27me3 repressive mark in the wild type (*AG*, *AP3*, *FLC*, and *LFY*; Turck et al., 2007).

Another gene found derepressed in the *icu2-1* mutant, *WUS*, is known to be regulated by the *FAS1* and *FAS2* chromatin assembling factors, which are related with chromatin packaging and DNA replication (Kaya et al., 2001). This suggests that *WUS*, an important meristematic gene, might also be regulated by chromatin-mediated gene silencing. Indeed, *WUS* is overexpressed as a consequence of loss of function of the *GCN5* gene, which encodes a histone acetyltransferase in *Arabidopsis* (Bertrand et al., 2003). Unexpectedly, we did not find the phenotypic traits characteristic of *WUS* overexpression, perhaps because the overexpression of other genes suppressed its effects. Our results bring to mind those obtained by other authors on the repression of homeotic genes in *Drosophila* and mammals and that of mating-type genes in yeasts and reinforce previous results indicating that floral transition, the major developmental switch in plant life, is controlled mainly by chromatin-mediated gene silencing (reviewed in He and Amasino, 2005; Reyes, 2006).

METHODS

Plant Material and Culture Conditions

Unless otherwise stated, all the mutations used in this work were loss of function and recessive. The *icu2-1* (N329) mutant (which we initially named *icu2* in Serrano-Cartagena et al., 2000) and its corresponding wild type, En-2 (N1138), as well as the *ag-1* (NW25; in the L*er* genetic background), *tfl2-2* (N3797; Col), *clf-2* (N290; L*er*), *ft-1* (N56; L*er*), *fas1-1* (N265; En-2), and *fas2-1* (N266; L*er*) lines, were provided by the Nottingham Arabidopsis Stock Centre. The *icu2-2* (in the Col genetic background), *icu2-3* (L*er*) and *emf2-5* (L*er*) mutants, and the *pAG-I:GUS* (No-0) and *gTFL2:GFP* (Col) transgenic lines were provided by GABI-Kat (http://www.mpiz-koeln.mpg.de/GABI-Kat/), Jonathan Clarke, Nobumasa Yoshida, Justin Goodrich, and Koji Goto, respectively.

Plants were grown in sterile (in 150-mm diameter Petri plates containing 100 mL of Murashige and Skoog agar medium, including 1% sucrose) or nonsterile (in pots containing a 2:2:1 mixture of perlite, vermiculite, and sphagnum moss) conditions at 20 ± 1°C, 60 to 70% relative humidity, and continuous illumination of 7000 lx, as described by Ponce et al. (1998). Sterile cultures were performed at a density of 100 regularly spaced seeds per plate in Conviron TC16 tissue culture chambers, and the plants were either collected to be studied or transferred to soil 21 d after sowing. When required, culture media were supplemented with 25 μg/mL of kanamycin or 10 μg/mL of sulfadiazine.

Sequencing

The synthetic oligonucleotides used for cycle sequencing (Table 2) were bought from Applied Biosystems or from Sigma-Genosys. The sequences of the wild-type En-2 and mutant alleles of the *ICU2* gene were obtained from both strands of the products of PCR amplifications of overlapping segments of the At5g67100 gene, whose wild-type Col-0 sequence was already available. Sequencing reactions were performed with ABI PRISM BigDye Terminator Cycle Sequencing kits in 5-μL reaction volumes, and sequencing electrophoreses were performed on an ABI PRISM 3100 Genetic Analyzer as described by Pérez-Pérez et al. (2004).

For bisulfite sequencing, genomic DNA was extracted from 21-d-old plants and bisulfite treated using the EZ DNA Methylation-Gold kit (Zymo Research; D5005) and the following reaction conditions: 10 min at 98°C, 10 min at 53°C, eight cycles consisting of 6 min at 53°C, and 30 min at 37°C, and a final step of 4°C. A 2-μL aliquot of bisulfite-treated DNA was used for each PCR amplification. Primer design (Table 2) and PCR conditions were similar to those previously described (Clark et al., 1994). PCR products were cloned using the TOPO TA cloning kit (Invitrogen). Ten to fifteen individual clones were sequenced for each experiment.

Complementation of the *icu2-1* Mutation

A 9467-bp DNA molecule, encompassing the whole *ICU2* transcription unit, was PCR amplified in 50-μL reaction mixes using K21H1 transformation-competent artificial chromosome as a template and the primers shown in Table 2, whose 5′ tails included *Not*I and *Sal*I restriction sites. The Expand Long Template PCR system (Roche) was used following the indications of the manufacturer and a polymerization time of 11 min. The PCR product obtained was digested with *Not*I and *Sal*I and cloned into the pGreenII0179 vector (Hellens et al., 2000). Competent *Escherichia coli* DH5α cells were transformed, and transformants were isolated on Luria-Bertani plates supplemented with 25 μg/mL of kanamycin, 0.25 mg/mL of X-Gal, and 0.04 mg/mL of isopropylthio-β-galactoside and tested by PCR for the presence of the construct. Plasmid DNA was isolated from positive clones and used to transform competent *Agrobacterium tumefaciens* C58C1 cells carrying the pSoup helper plasmid (Hellens et al., 2000). *Agrobacterium* transformants were selected on Luria-Bertani medium supplemented with 25 μg/mL of kanamycin and 5 μg/mL of tetracycline. Liquid cultures of the positives clones were used for in planta transformations of *Arabidopsis thaliana* wild-type and mutant plants (Bechtold and Pelletier, 1998). For the isolation of transformant plants, T2 seeds were sown in agar plates supplemented with 40 μg/mL of hygromycin. The presence of the transgene in the putative transformants was verified by PCR.

GUS Staining and GFP Visualization

Homozygotes for either the *gTFL2:GFP* or *pAG-I:GUS* transgene were crossed to mutant *icu2-1/icu2-1* and wild-type En-2 plants and their F1 allowed to selfpollinate. F2 plants carrying the transgene were selected in 25 μg/mL of kanamycin-supplemented plates. For GUS analyses, 21-d-old plants carrying the *pAG-I:GUS* transgene in wild-type and *icu2-1/icu2-1* backgrounds were collected and treated with 90% acetone for 15 min on ice. Samples were then washed with 100 mM sodium phosphate buffer, pH 7.0, containing 3 mM $K_4Fe(CN)_6$, 3 mM $K_3Fe(CN)_6$, and 0.1% Triton X-100 for 2 min on ice and then covered with 1 mM 5-bromo-4-chloro-3-indolyl β-D-glucuronide in the same buffer and incubated overnight at 37°C. After staining, leaves were cleared in an ethanol series. For GFP visualization, vegetative leaves of the 4th and 5th nodes were excised from 21-d-old plants carrying the *gTFL2:GFP* construct, mounted in water on slides, and directly observed by confocal laser scanning microscopy in a Leica TCS-NT microscope equipped with FITC/TRITC filters.

Real-Time QRT-PCR

QRT-PCR amplifications and measurements were performed as described by Pérez-Pérez et al. (2004) in an ABI PRISM 7000 sequence detection system. For each of the genes under study, a primer pair was designed (Table 2) to amplify a product of ~100 bp. To avoid amplification of genomic DNA, the 5′ and 3′ ends from each pair matched the sequences of two adjacent exons.

Plants were collected 21 d after sowing, frozen in liquid N_2, and ground in RNase-free conditions. RNA was extracted with the Qiagen RNeasy plant mini kit, and finally resuspended in 88 μL of RNase-free water and treated with DNaseI at 37°C for 30 min. RNA was then precipitated and resuspended in 40 μL of RNase-free water. Three to five micrograms of the RNA solution obtained were reverse transcribed using SuperScript II reverse transcriptase (Gibco BRL) following the manufacturer's instructions. One microliter of the resulting cDNA solution was used as template in a 25-μL QRT-PCR reaction mix, which included 12.5 μL of the SYBR-Green PCR master mix (Applied Biosystems) and 0.4 μM of primers. Relative quantification of gene expression was performed using the $2^{-\Delta\Delta C_T}$ or comparative C_T method (Livak and Schmittgen, 2001). Reactions were made in triplicate, and the expression levels were normalized using the C_T values obtained for the *OTC* housekeeping gene (Quesada et al., 1999), which was used as an internal reference gene (Cnops et al., 2004; Pérez-Pérez et al., 2004).

Pull-Down Assays

TFL2 cDNA was amplified from 5-d-old seedling mRNA using the Superscript III one-step RT system (Invitrogen) and specific primers spanning from the ATG to the stop codons. The cDNA was cloned in the Gateway-compatible vector D221 (Invitrogen). Afterwards, the cDNA was cloned into the pGEX gateway–adapted vector using the Gateway recombination protocol and introduced into the BL21 bacterial strain to express the recombinant GST or GST-TFL2 proteins under standard conditions. The recombinant proteins were bound to Glutathione sepharose beads (Amersham) and washed extensively with PBS-0.1% Tween 20. The amount of protein bound to beads was quantified by resolving the proteins in SDS-PAGE and staining the gel with SYPRO Ruby (Invitrogen).

The *ICU2* wild-type (En-2) and *icu2-1* mutant alleles were cloned as described for *TFL2*, the only exception being that only a segment of the full-length cDNA from nucleotide position 2041 after the ATG to the stop codon was cloned. The wild-type and mutant fragments were named *ICU2-ct* and *icu2-1-ct*, respectively. Both of them contained the region encoding the putative TFL2 binding domain, as well as that including the *icu2-1* mutation (in the *icu2-1-ct* fragment), and were cloned into pDEST17 (Invitrogen) and used for in vitro translation with the Wheat Germ system (Promega) in the presence of ^{35}S-Met following the instructions of the manufacturer.

For the pull-down assays, 1 μg of GST or GST-TFL2 bound to Glutathione sepharose beads (GE Healthcare) was incubated with the

^{35}S-labeled protein in PBS-0.1% Tween 20 at 4°C for 3 h. Afterwards, the beads were washed four times during 15 min with 1.5 mL of PBS-0.2% Tween 20. Proteins were resolved on an SDS-PAGE/8% bis-acrylamide gel, and the ^{35}S-products were detected by autoradiography.

ChIP Assay

ChIP was performed according to the protocol in the EpiQuik Plant ChIP kit manual (Epigentek) using 2-week-old En-2 and *icu2-1/icu2-1* seedlings and the following antibodies: anti-dimethyl H3K9 (Upstate Biotechnology), anti-trimethyl-H3K27 (Lindroth et al., 2004), anti-acetyl-H3, anti-acetyl-H3K9, and anti-acetyl-H3K14. We used the *OTC* housekeeping gene for normalization (Quesada et al., 1999). Semiquantitative PCR values were obtained as described by Schubert et al. (2006).

Accession Numbers

The Arabidopsis Genome Initiative locus identifiers for the genes identified and/or analyzed in this study are as follows: *AP1*, At1g69120; *AP3*, At3g54340; *CAL*, At1g26310; *CLF*, At2g23380; *EMF2*, At5g51230; *FAS1*, At1g65470; *FAS2*, At5g64630; *FLC*, At5g10140; *FUL*, At5g60910; *ICU2*, At5g67100; *LFY*, At5g61850; *OTC*, At1g75330; *PI*, At5g20240; *SEP3*, At1g24260; *SOC1*, At2g45660; and *WUS*, At2g17950.

ACKNOWLEDGMENTS

We thank the Nottingham Arabidopsis Stock Centre, GABI-Kat, J. Clarke, N. Yoshida, J. Goodrich, and K. Goto for providing seeds; C. Gutiérrez, H. Candela, J.M. Pérez-Pérez, V. Quesada, P. Robles, and three anonymous referees for comments on the manuscript; J.M. Serrano, V. García, and T. Trujillo for technical assistance; and A. Martínez-Laborda for his help in the low-resolution mapping of *ICU2* in the MBK5-K8K14 interval. This work was supported by fellowships (to J.M.B. and R.G.-B.) and grants (BMC2002-02840 and BMC2005-01031 to J.L.M., BMC2003-09763 to M.R.P., and BIO2004-01749 to J.C.P.) from the Ministerio de Educación y Ciencia of Spain.

Received July 11, 2007; revised August 5, 2007; accepted August 22, 2007; published September 14, 2007.

REFERENCES

Ahmad, K., and Henikoff, S. (2002). Epigenetic consequences of nucleosome dynamics. Cell **111:** 281–284.

Ahmed, S., Saini, S., Arora, S., and Singh, J. (2001). Chromodomain protein Swi6-mediated role of DNA polymerase alpha in establishment of silencing in fission yeast. J. Biol. Chem. **276:** 47814–47821.

Ayyanathan, K., Lechner, M.S., Bell, P., Maul, G.G., Schultz, D.C., Yamada, Y., Tanaka, K., Torigoe, K., and Rauscher III, F.J. (2003). Regulated recruitment of HP1 to a euchromatic gene induces mitotically heritable, epigenetic gene silencing: A mammalian cell culture model of gene variegation. Genes Dev. **17:** 1855–1869.

Bannister, A.J., Zegerman, P., Partridge, J.F., Miska, E.A., Thomas, J.O., Allshire, R.C., and Kouzarides, T. (2001). Selective recognition of methylated lysine 9 on histone H3 by the HP1 chromo domain. Nature **410:** 120–124.

Bastow, R., Mylne, J.S., Lister, C., Lippman, Z., Martienssen, R.A., and Dean, C. (2004). Vernalization requires epigenetic silencing of *FLC* by histone methylation. Nature **427:** 164–167.

Bates, P.A., Kelley, L.A., MacCallum, R.M., and Sternberg, M.J.E. (2001). Enhancement of protein modelling by human intervention in applying the automatic programs 3D-JIGSAW and 3D-PSSM. Proteins **5:** 39–46.

Bechtold, N., and Pelletier, G. (1998). In planta *Agrobacterium*-mediated transformation of adult *Arabidopsis thaliana* plants by vacuum infiltration. Methods Mol. Biol. **82:** 259–266.

Bertrand, C., Bergounioux, C., Domenichini, S., Delarue, M., and Zhou, D.X. (2003). *Arabidopsis* histone acetyltransferase AtGCN5 regulates the floral meristem activity through the *WUSCHEL/AGAMOUS* pathway. J. Biol. Chem. **278:** 28246–28251.

Biswas, S.B., Khopde, S.M., Zhu, F.X., and Biswas, E.E. (2003). Subunit interactions in the assembly of *Saccharomyces cerevisiae* DNA polymerase alpha. Nucleic Acids Res. **31:** 2056–2065.

Bouvier, D., Pignede, G., Damagnez, V., Tillit, J., de Recondo, A.M., and Baldacci, G. (1992). DNA polymerase alpha in the fission yeast *Schizosaccharomyces pombe*: Identification and tracing of the catalytic subunit during the cell cycle. Exp. Cell Res. **198:** 183–190.

Bowman, J.L., Alvarez, J., Weigel, D., Meyerowitz, E.M., and Smyth, D.R. (1993). Control of flower development in *Arabidopsis thaliana* by *APETALA1* and interacting genes. Development **119:** 721–743.

Bowman, J.L., Smyth, D.R., and Meyerowitz, E.M. (1989). Genes directing flower development in *Arabidopsis.* Plant Cell **1:** 37–52.

Bowman, J.L., Smyth, D.R., and Meyerowitz, E.M. (1991). Genetic interactions among floral homeotic genes of *Arabidopsis.* Development **112:** 1–20.

Chaboute, M.E., Clement, B., Sekine, M., Philipps, G., and Chaubet-Gigot, N. (2000). Cell cycle regulation of the tobacco ribonucleotide reductase small subunit gene is mediated by E2F-like elements. Plant Cell **12:** 1987–2000.

Chanvivattana, Y., Bishopp, A., Schubert, D., Stock, C., Moon, Y.H., Sung, Z.R., and Goodrich, J. (2004). Interaction of Polycomb-group proteins controlling flowering in Arabidopsis. Development **131:** 5263–5276.

Chen, L., Cheng, J.C., Castle, L., and Sung, Z.R. (1997). *EMF* genes regulate *Arabidopsis* inflorescence development. Plant Cell **9:** 2011–2024.

Chen, X., and Meyerowitz, E.M. (1999). *HUA1* and *HUA2* are two members of the floral homeotic *AGAMOUS* pathway. Mol. Cell **3:** 349–360.

Clark, S., Harrison, J., Paul, C.L., and Frommer, M.R. (1994). High sensitivity mapping of methylated cytosines. Nucleic Acids Res. **22:** 2990–2997.

Cnops, G., Jover-Gil, S., Peters, J.L., Neyt, P., De Block, S., Robles, P., Ponce, M.R., Gerats, T., Micol, J.L., and Van Lijsebettens, M. (2004). The *rotunda2* mutants identify a role for the *LEUNIG* gene in vegetative leaf morphogenesis. J. Exp. Bot. **55:** 1529–1539.

Craig, J.M. (2004). Heterochromatin–many flavours, common themes. Bioessays **27:** 17–28.

Cunliffe, V.T. (2003). Memory by modification: The influence of chromatin structure on gene expression during vertebrate development. Gene **305:** 141–150.

Ehrenhofer-Murray, A.E. (2004). Chromatin dynamics at DNA replication, transcription and repair. Eur. J. Biochem. **271:** 2335–2349.

Elgin, S.C., and Grewal, S.I. (2003). Heterochromatin: Silence is golden. Curr. Biol. **13:** R895–R898.

Farrona, S., Hurtado, L., Bowman, J.L., and Reyes, J.C. (2004). The *Arabidopsis thaliana* SNF2 homolog AtBRM controls shoot development and flowering. Development **131:** 4965–4975.

Francis, N.J., and Kingston, R.E. (2001). Mechanisms of transcriptional memory. Nat. Rev. Mol. Cell Biol. **2:** 409–421.

Fransz, P.F., and de Jong, J.H. (2002). Chromatin dynamics in plants. Curr. Opin. Plant Biol. **5:** 560–567.

Fry, C.J., and Farnham, P.J. (1999). Context-dependent transcriptional regulation. J. Biol. Chem. **274:** 29583–29586.

Gaudin, V., Libault, M., Pouteau, S., Juul, T., Zhao, G., Lefebvre, D., and Grandjean, O. (2001). Mutations in *LIKE HETEROCHROMATIN*

PROTEIN 1 affect flowering time and plant architecture in *Arabidopsis.* Development **128:** 4847–4858.

Gendall, A.R., Levy, Y.Y., Wilson, A., and Dean, C. (2001). The *VERNALIZATION 2* gene mediates the epigenetic regulation of vernalization in *Arabidopsis.* Cell **107:** 525–535.

Gil, J., Bernard, D., and Peters, G. (2005). Role of polycomb group proteins in stem cell self-renewal and cancer. DNA Cell Biol. **24:** 117–125.

Gómez Roig, E., and Vázquez-Ramos, J.M. (2003). Maize DNA polymerase alpha is phosphorylated by a PCNA-associated cyclin/Cdk complex: Effect of benzyladenine. J. Plant Physiol. **160:** 983–990.

Goodrich, J., Puangsomlee, P., Martin, M., Long, D., Meyerowitz, E.M., and Coupland, G. (1997). A Polycomb-group gene regulates homeotic gene expression in *Arabidopsis.* Nature **386:** 44–51.

Grewal, S.I., and Elgin, S.C. (2002). Heterochromatin: New possibilities for the inheritance of structure. Curr. Opin. Genet. Dev. **12:** 178–187.

Grewal, S.I., and Moazed, D. (2003). Heterochromatin and epigenetic control of gene expression. Science **301:** 798–802.

Gu, Q., Ferrandiz, C., Yanofsky, M.F., and Martienssen, R. (1998). The *FRUITFULL* MADS-box gene mediates cell differentiation during *Arabidopsis* fruit development. Development **125:** 1509–1517.

He, Y., and Amasino, R.M. (2005). Role of chromatin modification in flowering-time control. Trends Plant Sci. **10:** 30–35.

Hellens, R.P., Edwards, E.A., Leyland, N.R., Bean, S., and Mullineaux, P.M. (2000). pGreen: A versatile and flexible binary Ti vector for *Agrobacterium*-mediated plant transformation. Plant Mol. Biol. **42:** 819–832.

Henikoff, S. (2005). Histone modifications: Combinatorial complexity or cumulative simplicity? Proc. Natl. Acad. Sci. USA **102:** 5308–5309.

Hirose, F., Yamaguchi, M., Nishida, Y., Masutani, M., Miyazawa, H., Hanaoka, F., and Matsukage, A. (1991). Structure and expression during development of *Drosophila melanogaster* gene for DNA polymerase alpha. Nucleic Acids Res. **19:** 4991–4998.

Hoek, M., and Stillman, B. (2003). Chromatin assembly factor 1 is essential and couples chromatin assembly to DNA replication *in vivo.* Proc. Natl. Acad. Sci. USA **100:** 12183–12188.

Hubscher, U., Maga, G., and Spadari, S. (2002). Eukaryotic DNA polymerases. Annu. Rev. Biochem. **71:** 133–163.

Irish, V.F., and Yamamoto, Y.T. (1995). Conservation of floral homeotic gene function between Arabidopsis and Antirrhinum. Plant Cell **7:** 1635–1644.

Jack, T., Brockman, L.L., and Meyerowitz, E.M. (1992). The homeotic gene *APETALA3* of *Arabidopsis thaliana* encodes a MADS box and is expressed in petals and stamens. Cell **68:** 683–697.

Jenik, P.D., Jurkuta, R.E., and Barton, M.K. (2005). Interactions between the cell cycle and embryonic patterning in *Arabidopsis* uncovered by a mutation in DNA polymerase epsilon. Plant Cell **17:** 3362–3377.

Kaya, H., Shibahara, K.I., Taoka, K.I., Iwabuchi, M., Stillman, B., and Araki, T. (2001). *FASCIATA* genes for chromatin assembly factor-1 in *Arabidopsis* maintain the cellular organization of apical meristems. Cell **104:** 131–142.

Kempin, S.A., Savidge, B., and Yanofsky, M.F. (1995). Molecular basis of the cauliflower phenotype in *Arabidopsis.* Science **267:** 522–525.

Kobayashi, Y., Kaya, H., Goto, K., Iwabuchi, M., and Araki, T. (1999). A pair of related genes with antagonistic roles in mediating flowering signals. Science **286:** 1960–1962.

Kornberg, A., and Baker, T. (1991). DNA Replication, 2nd ed. (New York: Freeman and Company).

Kotake, T., Takada, S., Nakahigashi, K., Ohto, M., and Goto, K. (2003). *Arabidopsis TERMINAL FLOWER 2* gene encodes a heterochromatin protein 1 homolog and represses both *FLOWERING LOCUS T* to regulate flowering time and several floral homeotic genes. Plant Cell Physiol. **44:** 555–564.

Lachner, M., O'Carroll, D., Rea, S., Mechtler, K., and Jenuwein, T. (2001). Methylation of histone H3 lysine 9 creates a binding site for HP1 proteins. Nature **410:** 116–120.

Larsson, A.S., Landberg, K., and Meeks-Wagner, D.R. (1998). The *TERMINAL FLOWER2* (*TFL2*) gene controls the reproductive transition and meristem identity in *Arabidopsis thaliana.* Genetics **149:** 597–605.

Laux, T., Mayer, K.F., Berger, J., and Jurgens, G. (1996). The *WUSCHEL* gene is required for shoot and floral meristem integrity in *Arabidopsis.* Development **122:** 87–96.

Lee, H., Suh, S., Park, E., Cho, E., Ahn, J.H., Kim, S., Lee, J.S., Kwon, Y.M., and Lee, I. (2000). The *AGAMOUS-LIKE 20* MADS domain protein integrates floral inductive pathways in *Arabidopsis.* Genes Dev. **14:** 2366–2376.

Leyser, H.M., and Furner, I.J. (1992). Characterization of three shoot apical meristem mutants of *Arabidopsis thaliana.* Development **116:** 397–403.

Li, Y., Rosso, M.G., Strizhov, N., Viehoever, P., and Weisshaar, B. (2003). GABI-Kat SimpleSearch: A flanking sequence tag (FST) database for the identification of T-DNA insertion mutants in *Arabidopsis thaliana.* Bioinformatics **19:** 1441–1442.

Limsirichaikul, S., Ogawa, M., Niimi, A., Iwai, S., Murate, T., Yoshida, S., and Suzuki, M. (2003). The Gly-952 residue of *Saccharomyces cerevisiae* DNA polymerase alpha is important in discriminating correct deoxyribonucleotides from incorrect ones. J. Biol. Chem. **278:** 19079–19086.

Lindroth, A.M., et al. (2004). Dual histone H3 methylation marks at lysines 9 and 27 required for interaction with CHROMOMETHYLASE3. EMBO J. **23:** 4286–4296.

Lippman, Z., and Martienssen, R. (2004). The role of RNA interference in heterochromatic silencing. Nature **431:** 364–370.

Liu, Y.G., Shirano, Y., Fukaki, H., Yanai, Y., Tasaka, M., Tabata, S., and Shibata, D. (1999). Complementation of plant mutants with large genomic DNA fragments by a transformation-competent artificial chromosome vector accelerates positional cloning. Proc. Natl. Acad. Sci. USA **96:** 6535–6540.

Livak, K.J., and Schmittgen, T.D. (2001). Analysis of relative gene expression data using real-time quantitative PCR and the $2^{-\Delta\Delta C_T}$ method. Methods **25:** 402–408.

Mandel, M.A., Gustafson-Brown, C., Savidge, B., and Yanofsky, M.F. (1992). Molecular characterization of the *Arabidopsis* floral homeotic gene *APETALA1.* Nature **360:** 273–277.

Mathieu, O., and Bender, J. (2004). RNA-directed DNA methylation. J. Cell Sci. **117:** 4881–4888.

McNairn, A.J., and Gilbert, D.M. (2003). Epigenomic replication: Linking epigenetics to DNA replication. Bioessays **25:** 647–656.

Michaels, S.D., and Amasino, R.M. (1999). *FLOWERING LOCUS C* encodes a novel MADS domain protein that acts as a repressor of flowering. Plant Cell **11:** 949–956.

Miyazawa, H., Izumi, M., Tada, S., Takada, R., Masutani, M., Ui, M., and Hanaoka, F. (1993). Molecular cloning of the cDNAs for the four subunits of mouse DNA polymerase alpha-primase complex and their gene expression during cell proliferation and the cell cycle. J. Biol. Chem. **268:** 8111–8122.

Moon, Y.H., Chen, L., Pan, R.L., Chang, H.S., Zhu, T., Maffeo, D.M., and Sung, Z.R. (2003). *EMF* genes maintain vegetative development by repressing the flower program in *Arabidopsis.* Plant Cell **15:** 681–693.

Murakami, H., and Okayama, H. (1995). A kinase from fission yeast responsible for blocking mitosis in S phase. Nature **374:** 817–819.

Murzina, N., Verreault, A., Laue, E., and Stillman, B. (1999). Heterochromatin dynamics in mouse cells: Interaction between chromatin assembly factor 1 and HP1 proteins. Mol. Cell **4:** 529–540.

Nakahigashi, K., Jasencakova, Z., Schubert, I., and Goto, K. (2005). The *Arabidopsis* HETEROCHROMATIN PROTEIN1 homolog (TERMINAL FLOWER2) silences genes within the euchromatic region but not

genes positioned in heterochromatin. Plant Cell Physiol. **46:** 1747–1756.

Nakayama, J., Allshire, R.C., Klar, A.J., and Grewal, S.I. (2001). A role for DNA polymerase α in epigenetic control of transcriptional silencing in fission yeast. EMBO J. **20:** 2857–2866.

Nakayama, J., Klar, A.J., and Grewal, S.I. (2000). A chromodomain protein, Swi6, performs imprinting functions in fission yeast during mitosis and meiosis. Cell **101:** 307–317.

Niimi, A., Limsirichaikul, S., Yoshida, S., Iwai, S., Masutani, C., Hanaoka, F., Kool, E.T., Nishiyama, Y., and Suzuki, M. (2004). Palm mutants in DNA polymerases alpha and eta alter DNA replication fidelity and translesion activity. Mol. Cell. Biol. **24:** 2734–2746.

Ogawa, M., Limsirichaikul, S., Niimi, A., Iwai, S., Yoshida, S., and Suzuki, M. (2003). Distinct function of conserved amino acids in the fingers of *Saccharomyces cerevisiae* DNA polymerase alpha. J. Biol. Chem. **278:** 19071–19078.

Otte, A.P., and Kwaks, T.H. (2003). Gene repression by Polycomb group protein complexes: A distinct complex for every occasion? Curr. Opin. Genet. Dev. **13:** 448–454.

Pak, D.T., Pflumm, M., Chesnokov, I., Huang, D.W., Kellum, R., Marr, J., Romanowski, P., and Botchan, M.R. (1997). Association of the origin recognition complex with heterochromatin and HP1 in higher eukaryotes. Cell **91:** 311–323.

Parenicova, L., de Folter, S., Kieffer, M., Horner, D.S., Favalli, C., Busscher, J., Cook, H.E., Ingram, R.M., Kater, M.M., Davies, B., Angenent, G.C., and Colombo, L. (2003). Molecular and phylogenetic analyses of the complete MADS-box transcription factor family in *Arabidopsis*: new openings to the MADS world. Plant Cell **15:** 1538–1551.

Paro, R., Strutt, H., and Cavalli, G. (1998). Heritable chromatin states induced by the Polycomb and trithorax group genes. Novartis Found. Symp. **214:** 51–61.

Pelaz, S., Ditta, G.S., Baumann, E., Wisman, E., and Yanofsky, M.F. (2000). B and C floral organ identity functions require *SEPALLATA* MADS-box genes. Nature **405:** 200–203.

Pérez-Pérez, J.M., Ponce, M.R., and Micol, J.L. (2004). The *ULTRACURVATA2* gene of *Arabidopsis* encodes an FK506-binding protein involved in auxin and brassinosteroid signaling. Plant Physiol. **134:** 101–117.

Peterson, C.L., and Laniel, M.A. (2004). Histones and histone modifications. Curr. Biol. **14:** R546–R551.

Piñeiro, M., Gomez-Mena, C., Schaffer, R., Martinez-Zapater, J.M., and Coupland, G. (2003). EARLY BOLTING IN SHORT DAYS is related to chromatin remodeling factors and regulates flowering in *Arabidopsis* by repressing *FT.* Plant Cell **15:** 1552–1562.

Ponce, M.R., Quesada, V., and Micol, J.L. (1998). Rapid discrimination of sequences flanking and within T-DNA insertions in the *Arabidopsis* genome. Plant J. **14:** 497–501.

Quesada, V., Ponce, M.R., and Micol, J.L. (1999). *OTC* and *AUL1*, two convergent and overlapping genes in the nuclear genome of *Arabidopsis thaliana.* FEBS Lett. **461:** 101–106.

Quivy, J.P., Roche, D., Kirschner, D., Tagami, H., Nakatani, Y., and Almouzni, G. (2004). A CAF-1 dependent pool of HP1 during heterochromatin duplication. EMBO J. **23:** 3516–3526.

Reyes, J.C. (2006). Chromatin modifiers that control plant development. Curr. Opin. Plant Biol. **9:** 21–27.

Reyes, J.C., and Grossniklaus, U. (2003). Diverse functions of Polycomb group proteins during plant development. Semin. Cell Dev. Biol. **14:** 77–84.

Ronceret, A., Guilleminot, J., Lincker, F., Gadea-Vacas, J., Delorme, V., Bechtold, N., Pelletier, G., Delseny, M., Chaboute, M.E., and Devic, M. (2005). Genetic analysis of two *Arabidopsis* DNA polymerase epsilon subunits during early embryogenesis. Plant J. **44:** 23–36.

Rosso, M.G., Li, Y., Strizhov, N., Reiss, B., Dekker, K., and Weisshaar, B. (2003). An *Arabidopsis thaliana* T-DNA mutagenized population (GABI-Kat) for flanking sequence tag-based reverse genetics. Plant Mol. Biol. **53:** 247–259.

Rothwell, P.J., and Waksman, G. (2005). Structure and mechanism of DNA polymerases. Adv. Protein Chem. **71:** 401–440.

Rountree, M.R., Bachman, K.E., Herman, J.G., and Baylin, S.B. (2001). DNA methylation, chromatin inheritance, and cancer. Oncogene **20:** 3156–3165.

Sarraf, S.A., and Stancheva, I. (2004). Methyl-CpG binding protein MBD1 couples histone H3 methylation at lysine 9 by SETDB1 to DNA replication and chromatin assembly. Mol. Cell **15:** 595–605.

Sayle, R.A., and Milner-White, E.J. (1995). RASMOL: Biomolecular graphics for all. Trends Biochem. Sci. **20:** 374.

Schönrock, N., Exner, V., Probst, A., Gruissem, W., and Hennig, L. (2006). Functional genomic analysis of CAF-1 mutants in *Arabidopsis thaliana.* J. Biol. Chem. **281:** 9560–9568.

Schubert, D., Clarenz, O., and Goodrich, J. (2005). Epigenetic control of plant development by Polycomb-group proteins. Curr. Opin. Plant Biol. **8:** 553–561.

Schubert, D., Primavesi, L., Bishopp, A., Roberts, G., Doonan, J., Jenuwein, T., and Goodrich, J. (2006). Silencing by plant Polycomb-group genes requires dispersed trimethylation of histone H3 at lysine 27. EMBO J. **25:** 4638–4649.

Serrano-Cartagena, J., Candela, H., Robles, P., Ponce, M.R., Pérez-Pérez, J.M., Piqueras, P., and Micol, J.L. (2000). Genetic analysis of *incurvata* mutants reveals three independent genetic operations at work in *Arabidopsis* leaf morphogenesis. Genetics **156:** 1363–1377.

Serrano-Cartagena, J., Robles, P., Ponce, M.R., and Micol, J.L. (1999). Genetic analysis of leaf form mutants from the *Arabidopsis* Information Service collection. Mol. Gen. Genet. **261:** 725–739.

Sieburth, L.E., and Meyerowitz, E.M. (1997). Molecular dissection of the *AGAMOUS* control region shows that cis elements for spatial regulation are located intragenically. Plant Cell **9:** 355–365.

Singh, J., and Klar, A.J. (1993). DNA polymerase-alpha is essential for mating-type switching in fission yeast. Nature **361:** 271–273.

Smothers, J.F., and Henikoff, S. (2000). The HP1 chromo shadow domain binds a consensus peptide pentamer. Curr. Biol. **10:** 27–30.

Soppe, W.J., Jasencakova, Z., Houben, A., Kakutani, T., Meister, A., Huang, M.S., Jacobsen, S.E., Schubert, I., and Fransz, P.F. (2002). DNA methylation controls histone H3 lysine 9 methylation and heterochromatin assembly in *Arabidopsis.* EMBO J. **21:** 6549–6559.

Teper-Bamnolker, P., and Samach, A. (2005). The flowering integrator FT regulates *SEPALLATA3* and *FRUITFULL* accumulation in *Arabidopsis* leaves. Plant Cell **17:** 2661–2675.

Thompson, J.D., Gibson, T.J., Plewniak, F., Jeanmougin, F., and Higgins, D.G. (1997). The CLUSTAL_X windows interface: Flexible strategies for multiple sequence alignment aided by quality analysis tools. Nucleic Acids Res. **25:** 4876–4882.

Turck, F., Roudier, F., Farrona, S., Martin-Magniette, M.L., Guillaume, E., Buisine, N., Gagnot, S., Martienssen, R.A., Coupland, G., and Colot, V. (2007). Arabidopsis TFL2/LHP1 specifically associates with genes marked by trimethylation of histone H3 Lysine 27. PLoS Genet. **3:** e86.

Uchiyama, M., and Wang, T.S. (2004). The B-subunit of DNA polymerase alpha-primase associates with the origin recognition complex for initiation of DNA replication. Mol. Cell. Biol. **24:** 7419–7434.

Vermaak, D., Ahmad, K., and Henikoff, S. (2003). Maintenance of chromatin states: An open-and-shut case. Curr. Opin. Cell Biol. **15:** 266–274.

Wagner, D., and Meyerowitz, E.M. (2002). SPLAYED, a novel SWI/SNF ATPase homolog, controls reproductive development in *Arabidopsis.* Curr. Biol. **12:** 85–94.

Wahl, A.F., Geis, A.M., Spain, B.H., Wong, S.W., Korn, D., and Wang, T.S. (1988). Gene expression of human DNA polymerase alpha during cell proliferation and the cell cycle. Mol. Cell. Biol. **8:** 5016–5025.

Wang, J., Sattar, A.K., Wang, C.C., Karam, J.D., Konigsberg, W.H., and Steitz, T.A. (1997). Crystal structure of a pol alpha family replication DNA polymerase from bacteriophage RB69. Cell **89:** 1087–1099.

Wang, T.S., Wong, S.W., and Korn, D. (1989). Human DNA polymerase alpha: Prredicted functional domains and relationships with viral DNA polymerases. FASEB J. **3:** 14–21.

Weigel, D., Alvarez, J., Smyth, D.R., Yanofsky, M.F., and Meyerowitz, E.M. (1992). *LEAFY* controls floral meristem identity in *Arabidopsis.* Cell **69:** 843–859.

Wong, S.W., Wahl, A.F., Yuan, P.M., Arai, N., Pearson, B.E., Arai, K., Korn, D., Hunkapiller, M.W., and Wang, T.S. (1998). Human DNA polymerase alpha gene expression is cell proliferation dependent and its primary structure is similar to both prokaryotic and eukaryotic replicative DNA polymerases. EMBO J. **7:** 37–47.

Yang, C.H., Chen, L.J., and Sung, Z.R. (1995). Genetic regulation of shoot development in Arabidopsis: Role of the EMF genes. Dev. Biol. **169:** 421–435.

Yanofsky, M.F., Ma, H., Bowman, J.L., Drews, G.N., Feldmann, K.A., and Meyerowitz, E.M. (1990). The protein encoded by the *Arabidopsis* homeotic gene *agamous* resembles transcription factors. Nature **346:** 35–39.

Yokoi, M., Ito, M., Izumi, M., Miyazawa, H., Nakai, H., and Hanaoka, F. (1997). Molecular cloning of the cDNA for the catalytic subunit of plant DNA polymerase alpha and its cell-cycle dependent expression. Genes Cells **2:** 695–709.

Yoshida, N., Yanai, Y., Chen, L., Kato, Y., Hiratsuka, J., Miwa, T., Sung, Z.R., and Takahashi, S. (2001). EMBRYONIC FLOWER2, a novel polycomb group protein homolog, mediates shoot development and flowering in *Arabidopsis.* Plant Cell **13:** 2471–2481.

Zhang, Z., Shibahara, K., and Stillman, B. (2000). PCNA connects DNA replication to epigenetic inheritance in yeast. Nature **408:** 221–225.

Zilberman, D., Cao, X., and Jacobsen, S.E. (2003). *ARGONAUTE4* control of locus-specific siRNA accumulation and DNA and histone methylation. Science **299:** 716–719.

Zimmermann, P., Hirsch-Hoffmann, M., Hennig, L., and Gruissem, W. (2004). GENEVESTIGATOR. Arabidopsis microarray database and analysis toolbox. Plant Physiol. **136:** 2621–2632.